THE WAKE STEERING NOZZLE: A NEW METHOD OF STEERING SUBMERSIBLES

Greg J. Schoenau, et al

New Hampshire University

Prepared for:

Advanced Research Projects Agency
Office of Naval Research

31 January 1974

FINAL REPORT

Submersible Maneuvering: The Wake Steering Nozzle - A New Method of Steering Submersibles

Sponsored by
Advanced Research Projects Agency
ARPA Order No. 1958
ONR Contract No. N00014-67-A-0158-0006

Dr. C.K. Taft Principal Investigator
603-868-5074
University of New Hampshire

February 1, 1972 - Contract Effect Date
August 31, 1973 - Contract Expiration Date

Scientific Officer - Program Director
Ocean Technology Programs, Ocean Science and
Technology Division, ONR
800 N. Quincy Street
Arlington, Va. 22217

The views and conclusions contained in this document are those of the authors and should not be interpreted as necessarily representing the official policies, either expressed or implied, of the Advanced Research Projects Agency or the U.S. Government.

Amount of Contract $65,112.00
Form Approved Budget Bureau No. 22-R0293

SECURITY CLASSIFICATION OF THIS PAGE (When Data Entered)

REPORT DOCUMENTATION PAGE		READ INSTRUCTIONS BEFORE COMPLETING FORM
1. REPORT NUMBER	2. GOVT ACCESSION NO.	3. RECIPIENT'S CATALOG NUMBER
4. TITLE (and Subtitle) The Wake Steering Nozzle: A New Method of Steering Submersibles		5. TYPE OF REPORT & PERIOD COVERED Final Report Feb.1/72 to Sept.1/73
		6. PERFORMING ORG. REPORT NUMBER
7. AUTHOR(s) Greg J. Schoenau and Charles K. Taft		8. CONTRACT OR GRANT NUMBER(s) N00014-67-A-0158-0006
9. PERFORMING ORGANIZATION NAME AND ADDRESS University of New Hampshire Durham, New Hampshire 03824		10. PROGRAM ELEMENT, PROJECT, TASK AREA & WORK UNIT NUMBERS NR 294 - 005
11. CONTROLLING OFFICE NAME AND ADDRESS Office of Naval Research Arlington, Virginia 22217		12. REPORT DATE January 31, 1974
		13. NUMBER OF PAGES 89
14. MONITORING AGENCY NAME & ADDRESS(if different from Controlling Office)		15. SECURITY CLASS. (of this report) Unclassified
		15a. DECLASSIFICATION/DOWNGRADING SCHEDULE

16. DISTRIBUTION STATEMENT (of this Report)

Approved for public release; distributors unlimited

17. DISTRIBUTION STATEMENT (of the abstract entered in Block 20, if different from Report)

18. SUPPLEMENTARY NOTES

19. KEY WORDS (Continue on reverse side if necessary and identify by block number)

Nozzle
Steering
Submersible
Thrust

20. ABSTRACT (Continue on reverse side if necessary and identify by block number)

A new method of steering submersibles is investigated. This method utilizes a conventional shrouded or nozzled propeller. Control ports are placed on the nozzle aft of the propeller plane connecting the inner and outer nozzle surface. Opening a control port causes the wake to deflect producing a steering force. The concept is demonstrated to be feasible over a range of propeller - nozzle combinations and operating conditions.

DD FORM 1 JAN 73 1473 EDITION OF 1 NOV 65 IS OBSOLETE
S/N 0102-014-6601 |

SECURITY CLASSIFICATION OF THIS PAGE (When Data Entered)

SUMMARY

A new method of steering submersibles is investigated. The method, termed wake steering, utilizes a shrouded or nozzled propeller which is a conventional axial or forward thruster on submersibles and other vessels. On the wake steering device control ports are located in the nozzle aft of the propeller plane connecting the inner and outer nozzle surface. The wake steering nozzle is designed so that the pressure inside the nozzle in the vicinity of the control port is lower than ambient. Thus, opening a control port induces flow into the nozzle causing the wake to separate producing a radial or steering thrust.

A series of tests were conducted on model propellers and nozzles at zero and nonzero forward velocities to investigate the wake steering concept. The principle parameters varied in these tests were the propeller type, nozzle inside surface aft of the propeller plane, and nozzle length.

The static or zero forward velocity tests revealed that highly divergent nozzles are required to develop the high radial thrusts necessary to maximize the steering effeciveness of the device. The wake of these more divergent nozzles had a tendency to separate when the control port was closed producing an erratic and undesirable radial or steering thrust. However, a number of nozzle and propeller combinations

were found which operated reliably. These were the longer nozzles operating with propellers which were midrange in pitch in the series tested.

Tests of the wake steering nozzle at forward velocity revealed that the reliability of performance of the device was improved over the static tests and that the radial thrust of the nozzle increased with forward velocity.

One of the propeller and nozzle combinations tested at forward velocity was used for comparison with some existing submersible propulsion and steering systems. The device was found to produce a much greater axial thrust at low advance ratios but was less efficient. It is felt that the efficiency can be significantly improved through optimization of the nozzle design. In terms of steering effectiveness, the wake steering nozzle was shown to be as effective as a conventional submersible steering device, a tiltable shroud. By mounting a wake steering nozzle on the bow of a submersible, in addition to one on the tail, the device can be considered a potential canditate for replacing the propulsion and steering system of a conventional submersible such as the DSRV which has a tiltable shroud, main propeller and four ducted thrusters.

Additional information test equipment and experimental results can be found in References 11, 12 and 15.

TABLE OF CONTENTS

		Page
Section 1	INTRODUCTION	1
Section 2	THE WAKE STEERING NOZZLE - STATIC TESTING	7
2.1	The WSN Test Facility	7
2.1.1	The Measurement System	7
2.1.2	Propellers and Nozzles	13
2.2	Dimensionless Numbers	17
2.3	Preliminary Experimental Investigation	20
2.4	Analytical Modelling of the Nozzle Flow Field	28
2.5	Experimental Investigation of Major Parameters	33
2.6	Summary	
Section 3	FORWARD VELOCITY TESTING OF THE WAKE STEERING NOZZLE	40
3.1	Forward Velocity Test Facilty	41
3.2	Effect of Forward Velocity on WSN Performance Characteristics	47
3.3	Radial Force Control: Preliminary Tests	54
3.4	Summary	55
Section 4	AN EVALUATION OF THE PROPULSION STEERING CHARACTERISTICS OF THE WAKE STEERING NOZZLE	58

4.1	The Propulsive Efficiency of the Wake Steering Nozzle	59
4.2	An Evaluation of the Steering Effectiveness of the Wake Steering Nozzle	62
4.3	A Proposed System for Hovering Control	67
4.4	Summary	69
Section 5	CONCLUSIONS AND RECOMMENDATIONS	70
	LIST OF REFERENCES	74

LIST OF FIGURES

Figure	Title	Page
1	The Propulsion and Steering System of the DSRV	2
2	The Wake Steering Nozzle	4
3	Proposed Submersible Propulsion and Steering System Using Two WSN	6
4	Nozzle Force and Moment Measurement System	9
5	Motor Control Circuit	11
6	Nozzle Variation System	12
7	Cross sections of Aluminum Nozzles a) Nozzle No.1 , b) Nozzle No.2	15
8	Identification of Nozzle Geometric Parameters	16
9	Thrust Versus Propeller Speed for Nozzle No.2	22
10	Rotation of the Thrust Vector	21
11	Closed Port Pressure Distribution for Nozzle No.2	24
12	Open Port Pressure Distribution for Nozzle No.2	25
13	Flow Field of the Wake Steering Nozzle a) Without Propeller Hub b) With Propeller Hub	29
14	Port Closed Axial Pressure Distribution for Nozzles No.1 and No.2 with Propeller No.2	32

Figure	Title	Page
15	Water Channel Used for Testing Forward Velocity Nozzles	42
16	The Basic Configuration of the Wake Steering Nozzles Used for the Forward Velocity Tests	42
17	Geometric Parameters of the Forward Velocity Wake Steering Nozzles a) Front Section b) Aft Section	45
18	Flow Pattern of Nozzle A3 with Propeller No.2 Observed by Injecting Air Bubbles at the Nozzle Exit a) All Ports Closed b) Top Port Open	46
19	Forward Velocity Test Results for Nozzle A3 with Propeller No.4	48
20	Forward Velocity Test Results for Nozzle A2 with Propellers No.2, 4, and5	49
21	Forward Velocity Test Results for Nozzle A3 with Propellers No.1, 2, 4, and 5	50
22	Steering Ratio Versus Advance Ratio for Nozzles A2 and A3 a) Nozzle A2 b) Nozzle A3	53
23	Effect on the Coefficient of Radial Thrust of Axial Location of the Control Port	56
24	A Comparison of the Axial Thrust Coefficient and Efficiency of the Wake Steering Nozzle and Nozzle 19a	60

Figure	Title	Page
25	Turning Circle Simulation of DSRV Comparing WSN and Tiltable Shroud	65
26	Simulated 90° Accelerated Turn Comparing Wake Steering Nozzle and Tiltable Shroud	66
27	Simulated 90° Decelerated Turn Comparing Wake Steering Nozzle and Tiltable Shroud	66
28	Thrust Vectors Obtained by Mounting WSN on the Tail and Bow of a Submersible	68

NOMENCLATURE

D - propeller/nozzle inside diameter, cm

F - force, nts

J - advance ratio

K_{TA} - axial thrust coefficient

K_{TR} - radial thrust coefficient

K_{TR-A} - steering ratio

K_p - pressure coefficient

K_Q - torque coefficient

L - nozzle length, cm

L_a - length of nozzle aft section, cm

L_p - length of propeller, cm

n - propeller speed, rev/sec

P - propeller pitch, cm

P_a - ambient pressure of fluid, nts/m^2

P_s - pressure at any point on nozzle surface a distance Z from nozzle entrance, nts/m^2

P_v - vapor pressure of fluid, nts/m^2

Q - torque, nts-m

r_h - radius of the propeller hub, cm

R_c - radius of curvature of nozzle aft section inside surface, cm

R_{co} - radius of curvature of nozzle aft section outside surface, cm

t_p - propeller blade thickness, cm

V - fluid velocity, m/sec

Z - axial distance along nozzle surface, cm

ρ - fluid density, kg/m^3

μ - fluid viscosity, $nts\text{-}sec/m^2$

θ_d - nozzle divergence angle, degrees

θ_r - angle of rotation of the thrust vector, degrees

η - efficiency

SUBMERSIBLE MANEUVERING

1. INTRODUCTION

There has been a recent expanded usage of small submersibles such as Alvin, Dolphin and Deep Quest for re--search, rescue and recovery operations. These Deep Submer--gence Vehicles (DSV) belong to a new class of submersibles. Characteristic of this group are mission requirements calling for control over precise spatial orientation and translation of the vehicle in all the six degrees of freedom. Precise positional navigation is essential for such operations as the search for and recovery of objects from the ocean bottom. With the resulting emphasis on control as opposed to speed, the DSV is generally equipped with more thrusters and steering surfaces than the fleet or attack submarines.(1-2)*

The propulsion-steering system of one of the more sophisticated submersibles, the U.S. Navy's Deep Submergence Rescue Vehicle (DSRV) is shown in Fig.1. The reversible main propeller provides for thrusts along the vehicle surge axis. The tiltable shroud provides yaw and pitch turning moments during cruising. For hovering maneuvers, the tiltable shroud is largely ineffective and the ducted thrusters are used to provide yaw and pitch moments as well as sway and heave forces.

* Numbers in brackets refer to references.

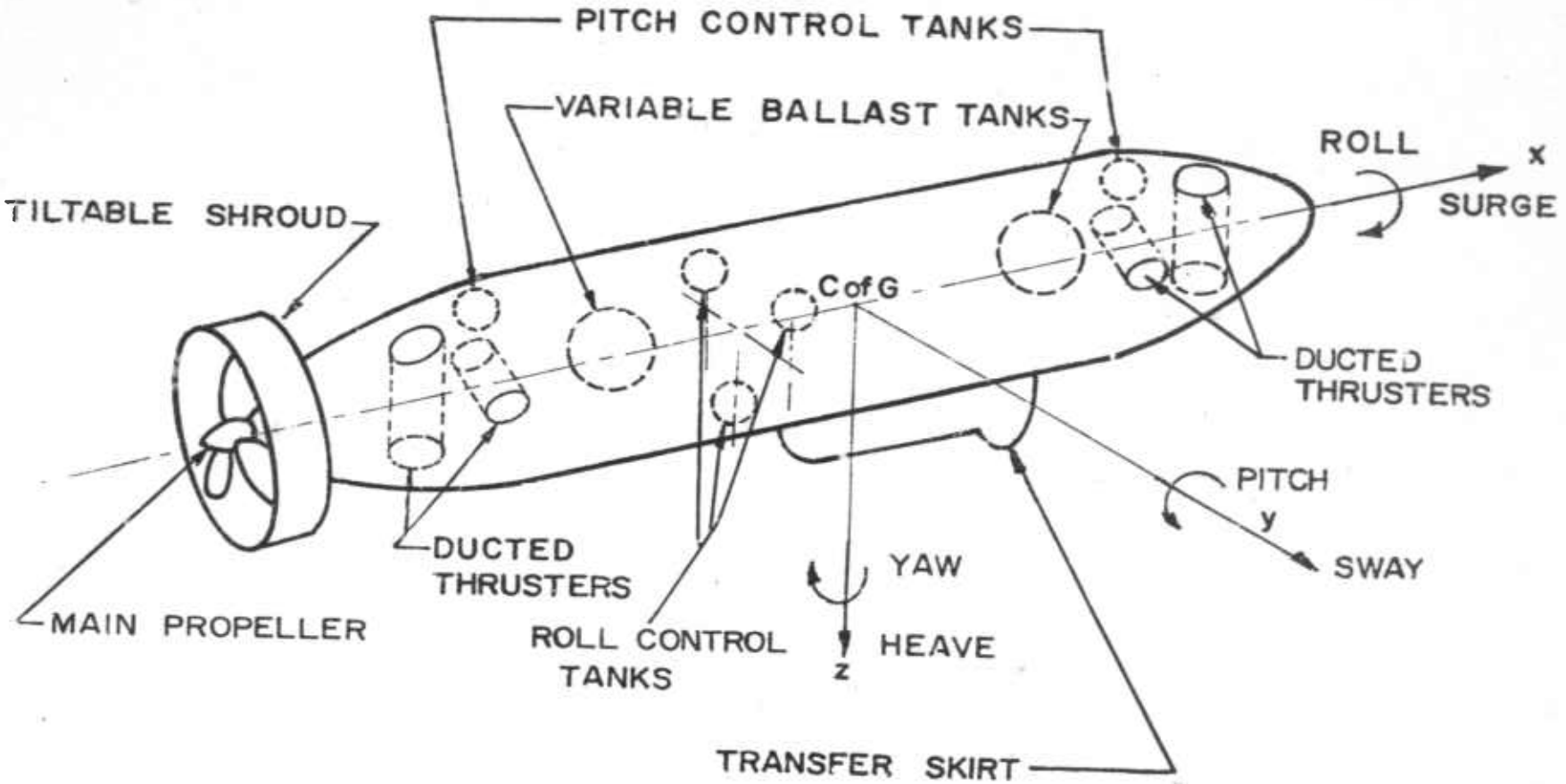

Fig.1 The Propulsion and Steering System of the DSRV

Steady state roll and pitch moments are achieved by pumping mercury between the tanks. Vehicle neutral buoyancy at any depth is achieved by controlling the amount of water in the variable ballast tanks.

The wake steering nozzle (WSN) is a new method of steering submersibles. It offers the potential of reducing the number of thrusters as compared with a conventional sys--tem while maintaining a comparable level of maneuverability and increasing vessel geometric symmetry. The WSN shown in Fig.2, consists of a propeller surrounded by an accelerating type flow shroud. This nozzle or shroud has the effect of increasing the water velocity through the duct in the region of the propeller,enabling the propeller to operate under a favorable loading criterion. The use of shrouded propellers as thrusters is not new and has been explored both experi--mentally and analytically.(3-8) What is unique about the WSN as proposed by Wozniak, Taft and Alperi, is its ability to develope a steering force as well as an axial thrust.(9-10) The concept is based on the fact that a shrouded propeller can be designed that has a pressure distribution downstream of the propeller plane which is lower than ambient pressure. Providing an open slot or control port downstream of the propeller thus allows flow to be induced into the shroud causing a separation of the wake from one side of the nozzle.

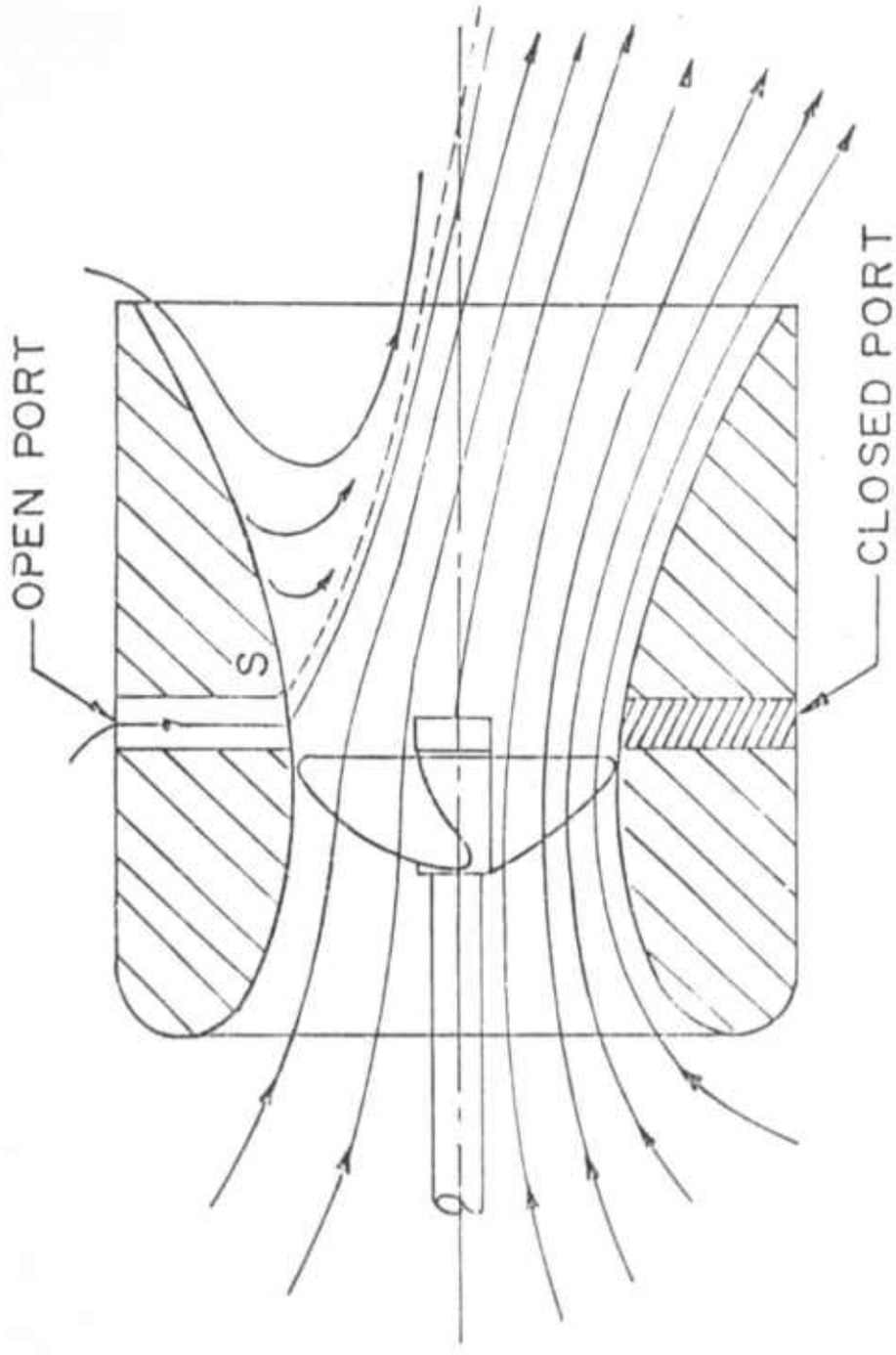

Fig.2 The Wake Steering Nozzle

This is illustrated by the streamlined pattern shown in Fig. 2. This results in an asymmetry in the pressure distribution inside the shroud producing a radial steering force. From an--other viewpoint, the wake is deflected through an angle rel--ative to the propeller axis causing a radial momentum force. Thus by locating a set of slots downstream from the propeller and opening and closing these slots the wake can be steered.

Assuming a strategy for controlling the direction of the wake, then two WSN mounted on a submersible, one fore and one aft, would provide the same capability to generate independent control forces and moments in each degree of free--dom as the thrusters now on the DSRV. The resulting increase in submersible fore to aft geometric symmetry is apparent in Fig.3 which shows configuration. The ability of the wake steer--ing shroud to generate steering forces at vessel zero forward velocity is an additional advantage over steering surfaces such as rudders.

The objective of the research on the WSN was to gain an improved understanding of the phenomena to enable assessment of its potential use in a propulsion-steering system for sub--mersibles. The performance of the WSN was evaluated experiment--ally at both zero and nonzero forward velocity. One of the prime advantages of the WSN over conventional steering surfaces is its ability to develop steering forces at zero forward velocity.

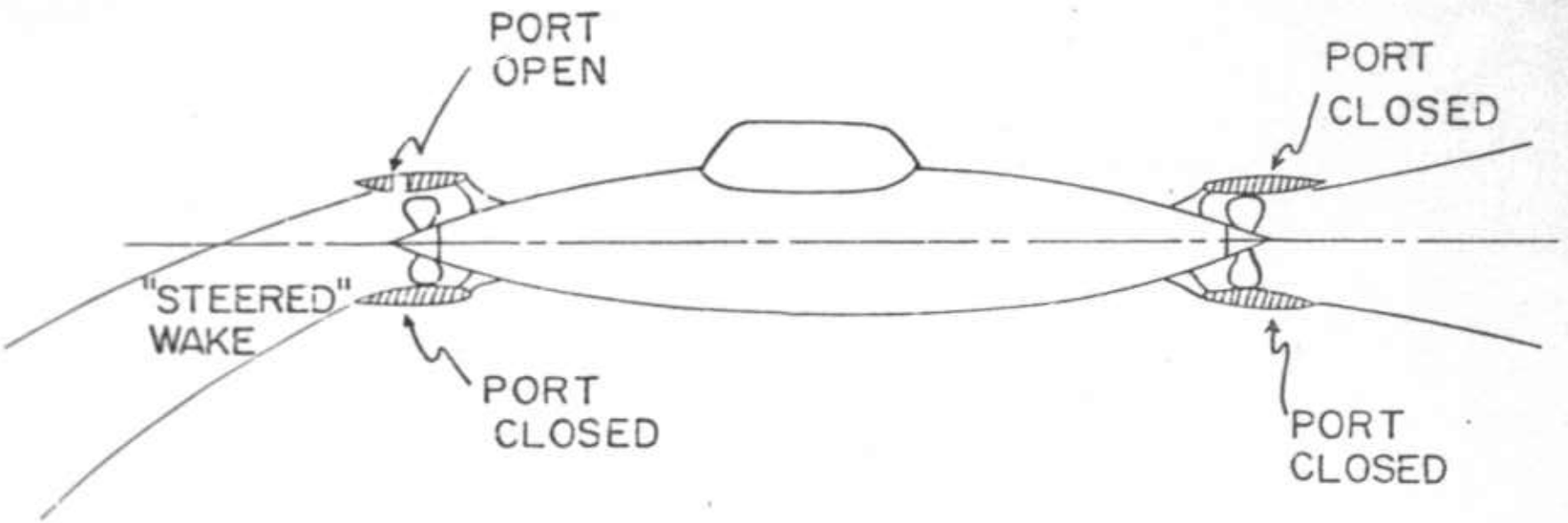

Fig.3 Proposed Submersible Propulsion and Steering System Using Two WSN

2. THE WAKE STEERING NOZZLE - STATIC TESTING

This section deals with the experimental investiga-tion of a number of geometric parameters of the WSN at zero forward velocity or static operation.

The experimental facility constructed for testing the WSN is described. Several nondimensional numbers are dev-eloped to enable a reduction of the data for comparison of the axial thrust characteristics of the WSN with those of conventional shrouded propellers.[4-5] A preliminary series of exploratory tests were run. These served to define a number of important parameters of shroud geometry which were invest-igated in a more extensive set of tests. Mathmatical model-ling of the observed flow field as an aid in guiding the experimental effort is also discussed.

2.1 The WSN Test Facility

2.1.1 The Measurement System

In the experimental system used by Wozniak, the axial and radial forces produced by a WSN were determined indirectly, using measurements of the pressure on the inside shroud surface.[9] These pressure measurements were converted to forces using a computer program which took into account

shroud shape. This method was time consuming and cumbersome. Our first task therefore was to develop a means for direct measurement of the forces being produced by a WSN.

To this end a five component dynamic force balance or dynamometer was designed and constructed.[11] It essentially consists of a vertical beam instrumented with strain gages. (See Fig.4.) The gages and associated instruments allow the axial force and the horizontal component of radial force to be measured and recorded as functions of time on an oscillograph. To completely specify the radial force, another component must be measured. This other component is obtained by repeating the test run and opening a port located at 90° from the first port. The two components are then added vectorially to determine the radial force magnitude and direction. In addition, the system can also measure and record all three moments. The beam is damped in the horizontal plane by two mechanical dampers manu--factured by Airpot Corporation mounted along axes orthogonal to each other. The WSN to be tested were mounted on the end of the beam and emmersed in a tank .914 meters by 2.44 meters with the water depth kept at about .6 meters. The tank was baffled to reduce recirculation eddies in the region of the shroud occurring as a result of the pumping action of the propeller and the constriction imposed by the tank.

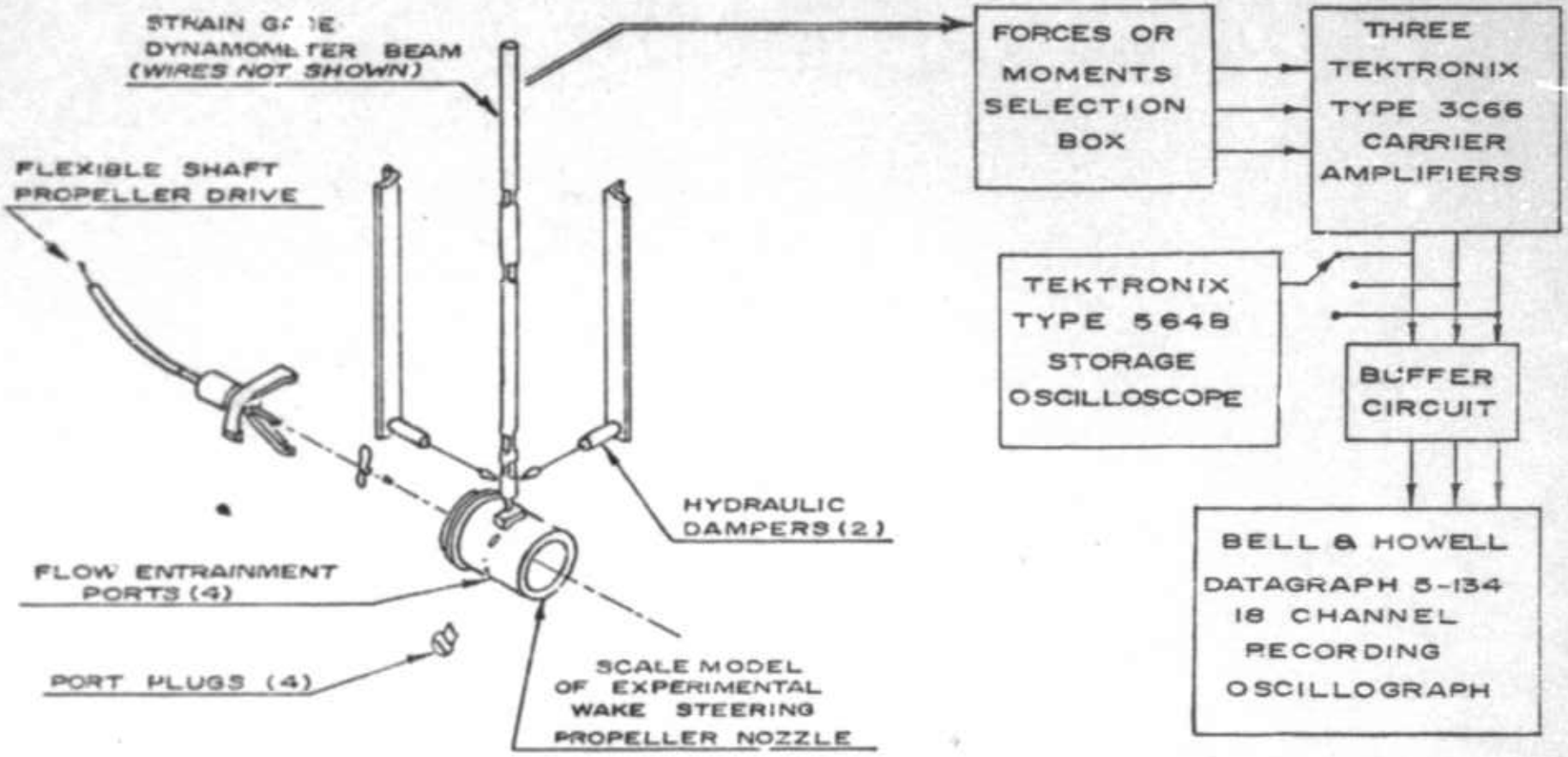

Fig. 4 Nozzle Force and Moment Measurement System

The propeller is driven by a DC motor through a flexible shaft. Propeller torque is measured by measuring and recording armature current on the oscillograph. Motor dynam--ometer tests were used to establish the relationship between armature current and propeller torque. Motor speed was con--trolled by varying the armature current with speed measured by a tachometer. A schematic of the motor control circuit is shown in Fig.5.

Pressures inside the aluminum shrouds were measured by means of a manometer bank connected to the shroud by tubing through the tank.

The aluminum shrouds were time consuming to make and difficult to machine. As a result, a special shroud holder was designed and constructed by Clark which enabled the shroud shape to be easily and rapidly changed. The shroud holder was mounted on the same dynamometers used for testing the aluminum shrouds. The system is shown in Fig.6 . The shroud holder has a cylindrical inner surface of fixed diameter in the region of the control port. This ring contains a port valve assembly which is rotatable. This valve is actuated by means of an air cylinder. The shroud surface fore and aft of the holder can be changed by switching inserts. These inserts are machined out of wax stiffened by a section of aluminum pipe. The machining of

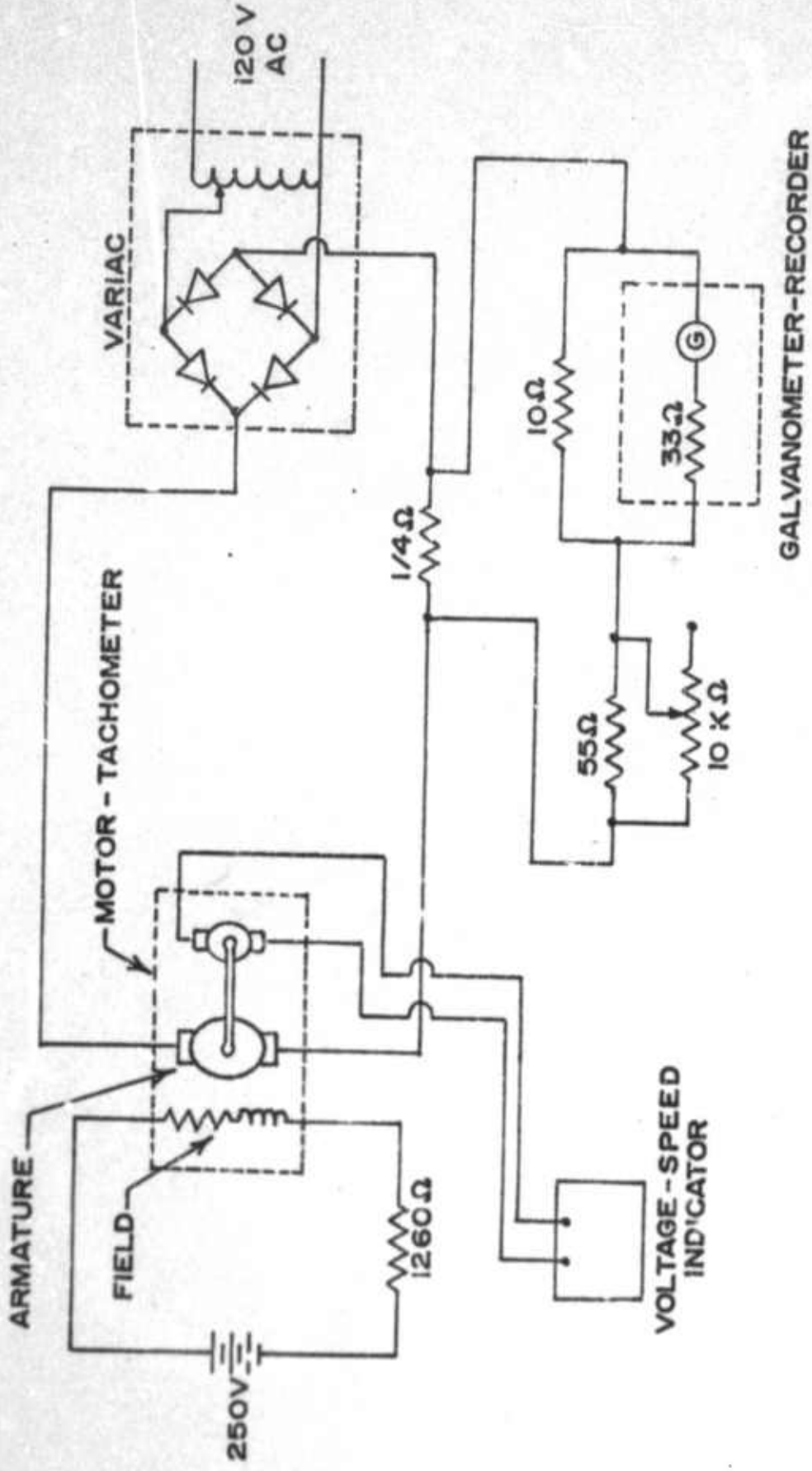

Fig.5 -Motor Control Circuit

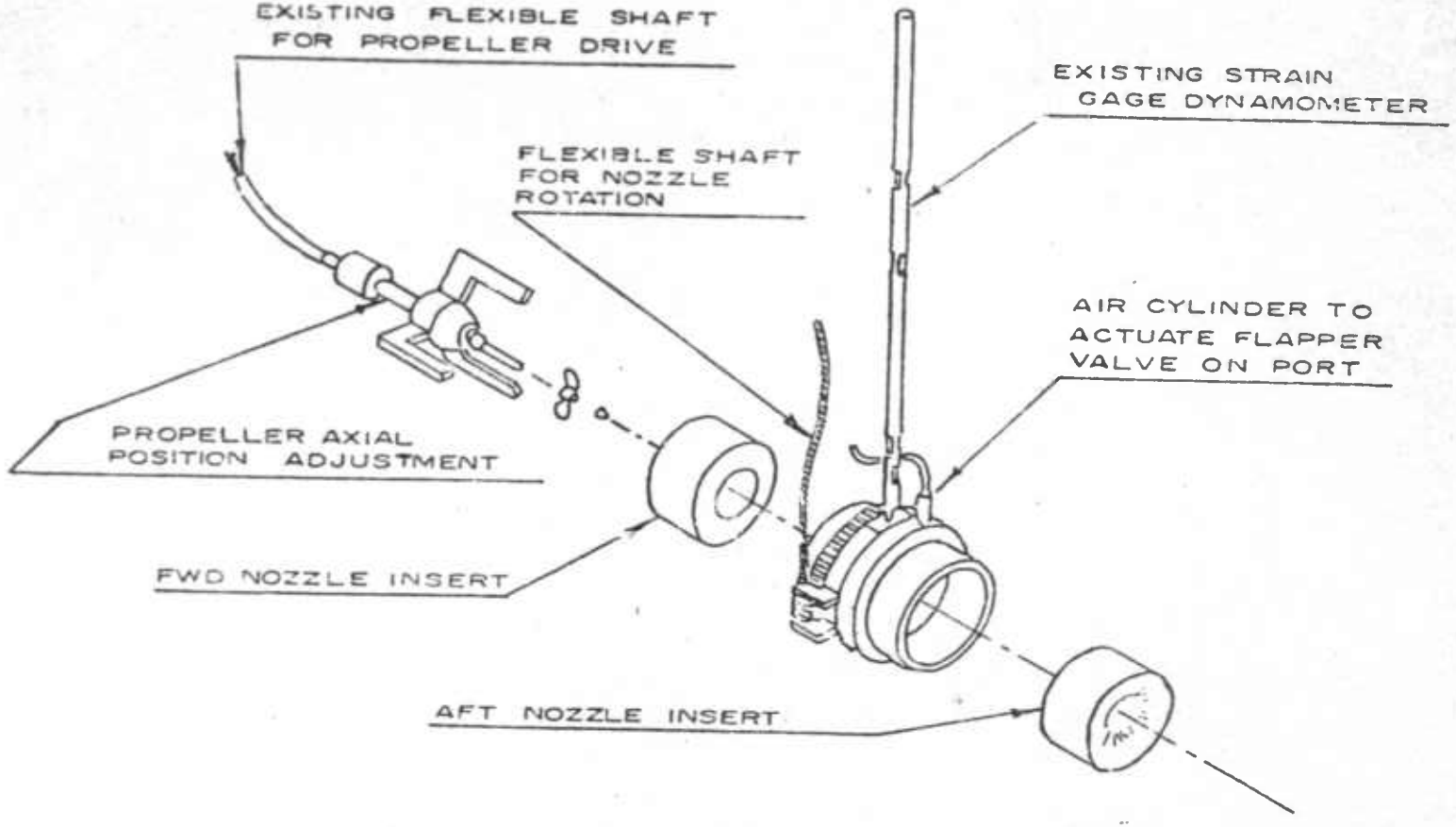

Fig.6 Nozzle Variation System

the wax was done on a lathe using a forming tool constructed from heavy gage sheet metal cut to the desired nozzle shape.

2.1.2 Propellers and Nozzles

A series of two bladed propellers were used. The principle difference between these propellers is in their pitch to diameter ratios which varied from 1.24 to 2.06 (measured at 7/10 the radius). The propellers also differed in blade length L_p, blade thickness t_p and propeller diameter D. The dimensions of the six propellers used in the tests are given in Table 1. Drawings showing the profiles of each of the propellers are contained in Reference 12.

The two aluminum nozzles tested, designated No.1 and No.2, are shown to full scale in Fig.7(a) and 7(b) resp--ectively. The inside shape of nozzle No.1 is based on nozzle No.32 developed by the Netherlands Ship Model Basin (4) and nozzle No.2 has the inside shape of an NACA-16-021 airfoil at zero angle of attack.(13)

Two series of wax nozzles were developed for extensive testing. Fig.8 identifies the parameters varied in this series of nozzles. This series utilized the shroud variation system and were therefore made up of fore and aft

TABLE 1

PROPELLER DIMENSIONS

Propellers	$2r_{p/D}$	$L_{p/D}$	$t_{p/D}$	P cm.
Prop. No.1				
D = 4.42 cm.	.930	.374	.014	5.34
r_h = .94 cm.	.818	.496	.022	5.52
	.702	.609	.034	5.50
P/D= 1.24	.585	.620	.040	5.50
	.468	.541	.041	5.50
	.351	.397	.039	5.41
Prop. No.2				
D = 4.42 cm.	.936	.316	.007	7.52
r_h = 1.00 cm.	.818	.487	.015	6.64
	.702	.607	.017	6.22
P/D= 1.41	.585	.620	.028	5.84
	.468	.541	.031	5.79
	.351	.458	.024	5.81
Prop. No.3				
D = 4.32 cm.	.936	.468	.022	7.09
r_h = 1.05 cm.	.818	.594	.032	7.16
	.702	.629	.029	7.06
P/D= 1.64	.585	.577	.043	7.11
	.468	.495	.043	7.08
	.351	.419	.049	6.64
Prop. No.4				
D = 4.42 cm.	.936	.346	.010	8.81
r_h = 1.03 cm.	.818	.462	.014	8.07
	.702	.475	.024	7.64
P/D= 1.73	.585	.449	.076	7.26
	.468	.402	.034	7.09
	.351	.348	.043	6.64
Prop. No.5				
D = 4.37 cm.	.936	.488	.020	8.76
r_h = 1.02 cm.	.818	.540	.034	8.58
	.702	.514	.036	8.36
P/D= 1.97	.585	.480	.036	8.12
	.468	.428	.052	8.68
	.351	.376	.051	8.26
Prop. No.6				
D = 4.42 cm.	.936	.316	.011	9.26
r_h = 1.06 cm.	.818	.445	.016	8.96
	.702	.513	.026	9.12
P/D= 2.06	.585	.474	.030	8.78
	.468	.439	.036	8.86
	.354	.372	.037	8.66

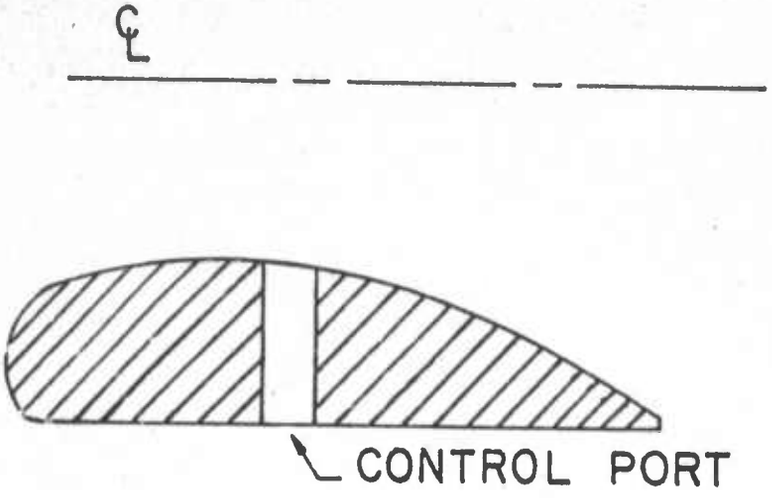

a) Nozzle No. 1

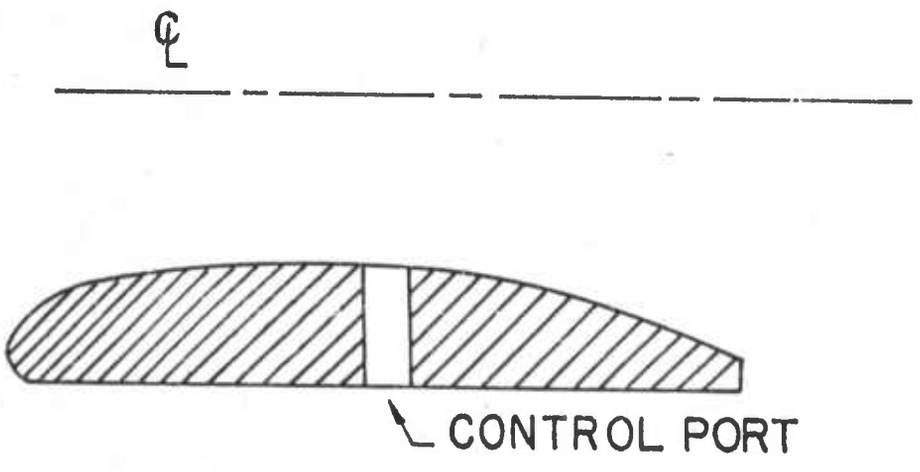

b) Nozzle No. 2

Fig. 7 Cross-sections of Aluminum Nozzles

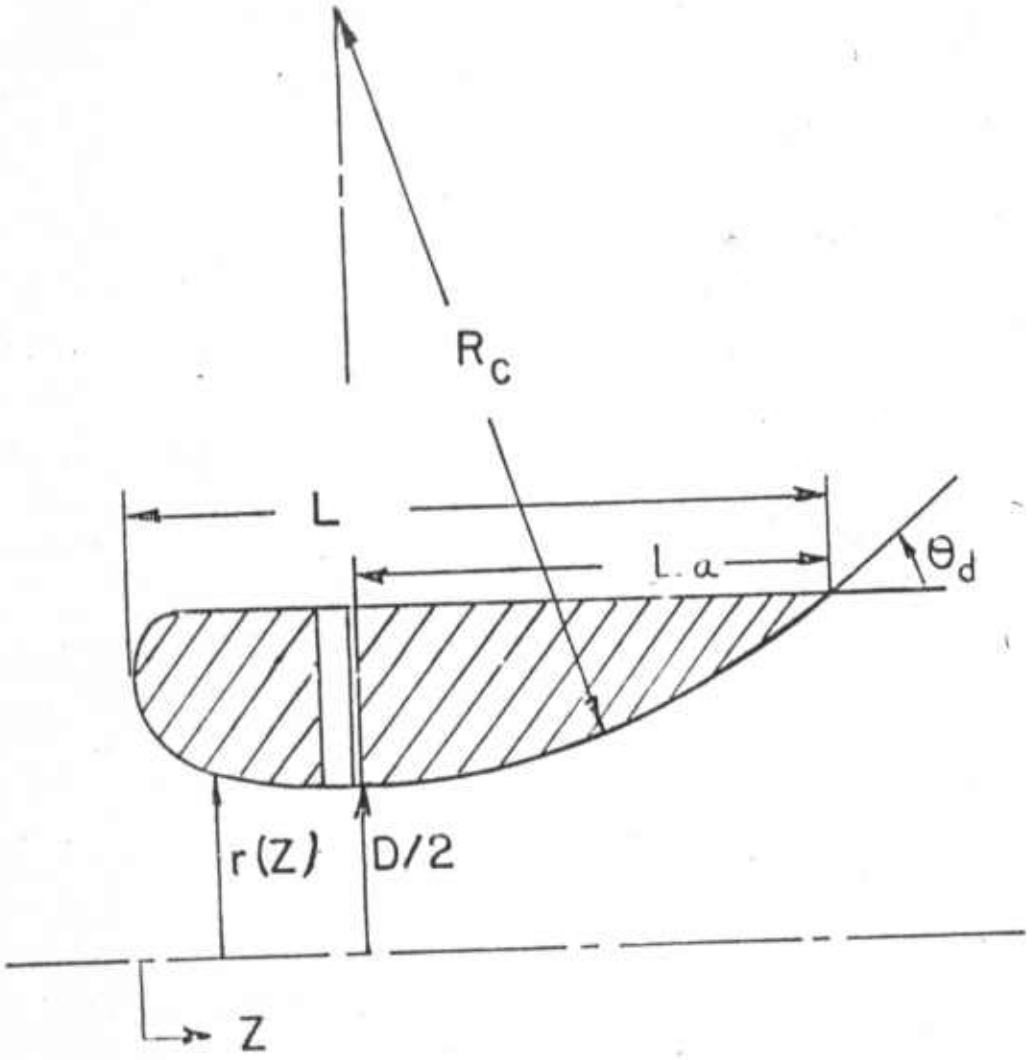

Fig.8 Identification of Nozzle Geometric Parameters

inserts machined from wax. Both series used the same fore insert having a length of 5.08 cm. and the same inside profile as aluminum nozzle No.2. The rear inserts of both series were varied as shown in Table 2. Series A was generated by varying the radius of curvature R_c and Series B by varying the length of the aft section L_a.

2.2 Dimensionless Numbers

To reduce the number of parameters to be varied in the testing and nondimensionalize the data, some dimensionless numbers are developed in this section.

TABLE 2

DESCRIPTION OF WAX NOZZLES

Nozzle Numbers	θ_d (Degrees)	$R_{c/D}$	$L_{a/D}$
Series A			
A1	12.5	5.28	1.14
A2	19.4	3.43	1.14
A3	22.9	2.93	1.14
A4	28.1	2.43	1.14
A5	31.5	2.19	1.14
Series B			
B1	12.5	2.19	0.47
B2	19.4	2.19	0.72
B3	22.9	2.19	0.85
B4	28.1	2.19	1.02
B5	31.5	2.19	1.14

D = 4.45 cm.

For a given propeller and nozzle design it can be shown that the thrust, torque and pressure difference between the inside and outside shroud surfaces of the nozzle are a function of the velocity of the nozzle relative to the fluid.

That is:

$$\text{Thrust} = F = g_1(V, n, D, \rho, \mu)$$

$$\text{Torque} = Q = g_2(V, n, D, \rho, \mu)$$

$$P_s - P_a = P = g_3(V, n, D, \rho, \mu, Z/D)$$

where V = velocity relative to the field

n = propeller rotational speed (rev./sec.)

D = propeller/shroud diameter

ρ = density of the fluid

μ = viscosity of the fluid

P_s = pressure at any point on the shroud a distance Z from the shroud entrance

P_a = ambient pressure of the fluid

P_v = vapor pressure of the fluid

A dimensional analysis yields:

$$F/\rho n^2 D^4 = \phi_1(V/nD, \rho nD^2/\mu, P_v/\rho n^2 D^2)$$

$$Q/\rho n^2 D^5 = \phi_2(V/nD, \rho nD^2/\mu, P_v/\rho n^2 D^2)$$

$$P_s/\rho n^2 D^2 = \phi_3(V/nD, \rho nD^2/\mu, P_v/\rho n^2 D^2, Z/D)$$

This is one set of dimensionless numbers, others are also possible.

In most submersible and ship designs, Reynolds number is very high so that the flow is essentially turb--ulent and independent of Reynolds number. In the testing program, Reynolds number based on tip speed = $\rho nD^2/\mu$, varied from $1.00(10)^5$ to $3.75(10)^5$ over a range of propeller speeds of interest indicating operation in a turbulent regime. In addition, the Cavitation number based on tip speed = $2(P_a-P_v)/(\rho n^2D^2)$ has a minimum value of 1.63 which is large enough to ensure that propeller cavitation is not occurring in the tests. Hence, the dimensionless equations can be simplified to

$$F/\rho n^2D^4 = \phi_1(V/nD)$$
$$Q/\rho n^2D^5 = \phi_2(V/nD)$$
$$R/\rho n^2D^2 = \phi_3(V/nD, Z/D)$$

where $F/\rho n^2D^4$ = coefficient of thrust, K_t

$Q/\rho n^2D^5$ = coefficient of torque, K_q

$R/\rho n^2D^2$ = coefficient of pressure, K_p

V/nD = coefficient of advance, J

as defined by previous researchers on shrouded propellers.[3-8]

The ratio of the radial to axial coefficients of thrust is a measure of the ability of the WSK to produce steering moments on a vessel and will be defined as the steer--ing ratio

$$K_{TR}/K_{TA} = \text{steering ratio, } K_{TR-A}$$

In practice, we would want this ratio to be as large as possible. The radial thrust obtained from the WSN is dependent on the axial thrust developed. Therefore, by maximizing this ratio, we minimize the space required for a submersible to turn thus increasing its maneuverability.

Another parameter of equal importance is the thruat--ing efficiency η of the WSN. This can be expressed in terms of the nondimensional coefficients as

$$\eta = J K_{TA}/2\pi K_Q$$

Since in this section we are concerned only with tests on the WSN at zero forward velocity, the advance coeffi--cient was zero throughout. Thus the thrust coefficient and pressure coefficient distribution along the nozzle inside surface characterize the static performance of a given WSN.

2.3 Preliminary Experimental Investigation

The axial and radial thrusts of aluminum nozzles No.1 and No.2 using propeller No.2, were measured with a control port open and closed. Analysis of the thrust data

reveals that the thrust very nearly varies with the square of propeller speed as was expected from the dimensional analysis. This is evident in Fig.9. The results also revealed that an angular displacement θ_r of the radial thrust vector relative to the open port occurs. The rotation occurs in the direction of propeller rotation according to Fig. 10.

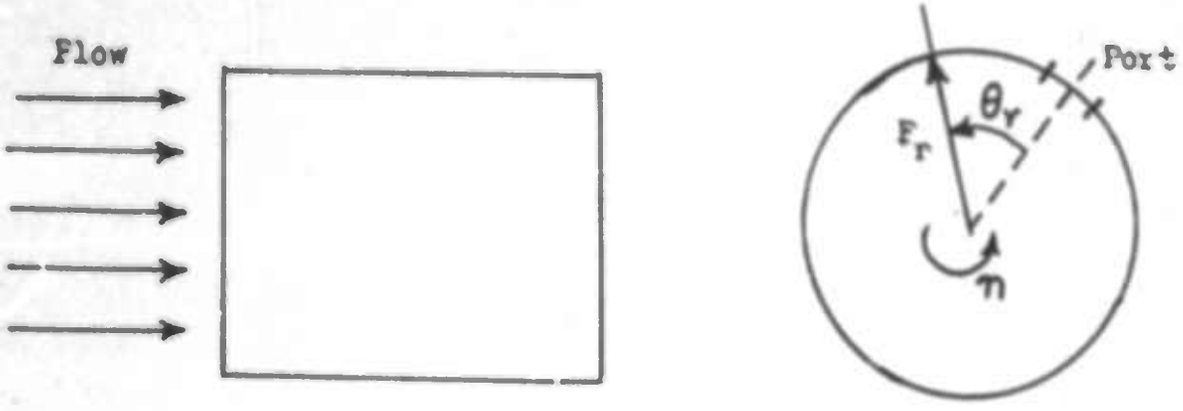

Fig.10 Rotation of the Thrust Vector

The relative angle of the thrust vector decreases only slightly with propeller speed. The results are summarized in Table 3.

TABLE 3

THRUST COEFFICIENTS FOR NOZZLE NO.1 AND NO.2

Nozzle	K_{TA}	K_{TR}	K_{TR-A}	θ_r 25 rev./sec	θ_r 90 rev./sec.
No.1	.71	.38	.54	22.4	18.0
No.2	.79	.28	.36	35.2	33.5

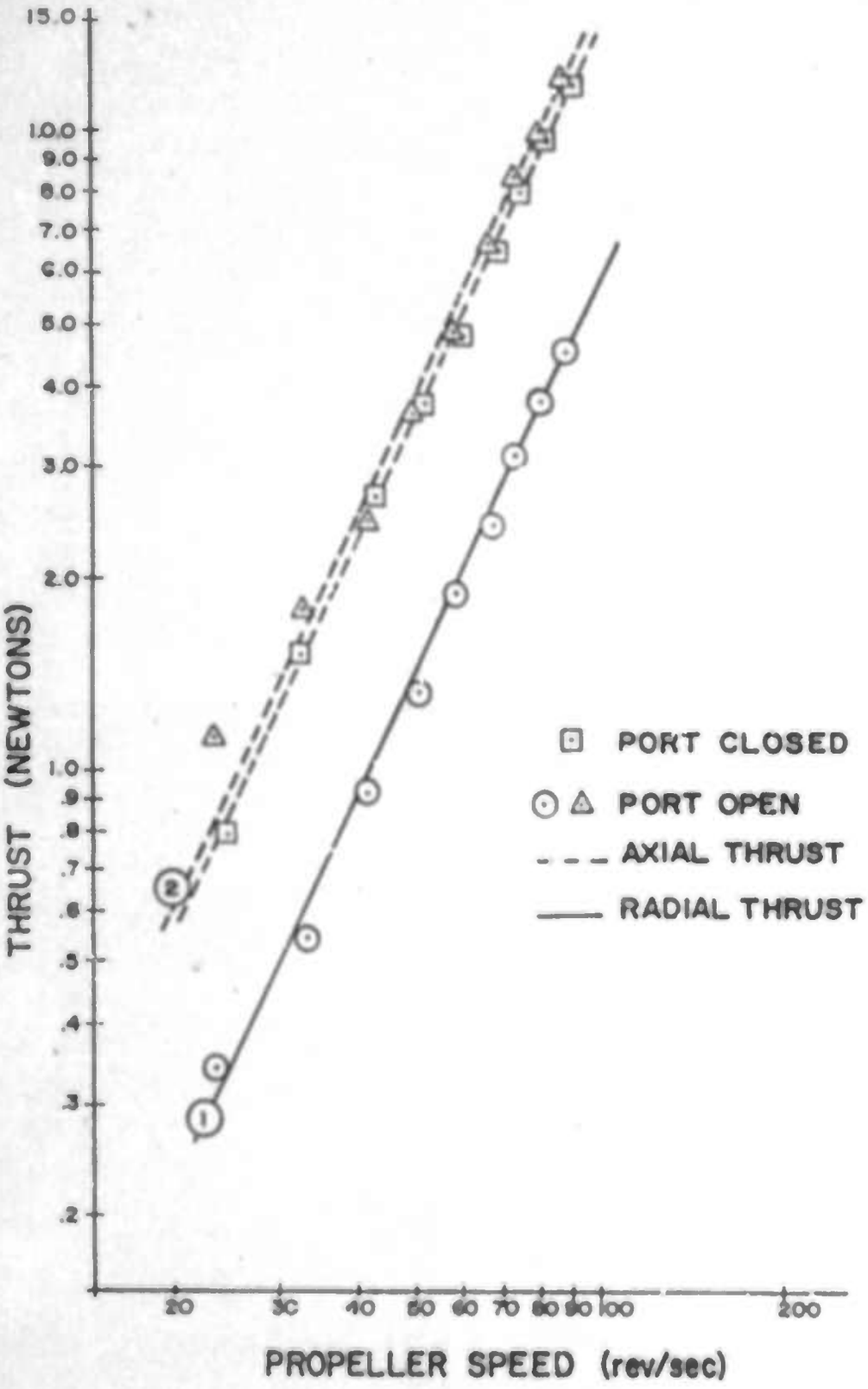

Fig.9 Thrust Versus Propeller Speed for Nozzle No.2

Moments about the three mutually perpendicular axes of nozzle No.2 were measured. These were found to be small and insignificant when compared with vessel turning moments produced by nozzle radial thrust and propeller torque. The measurement of the moments revealed that the point of location of the thrust vector was inside the aft section of the nozzle at $Z/L = .84$ and that the variation in location of this vector was less than $\pm$ 3.8% over the full range of propeller speed. (See Reference 12) hence, the errors in vessel turning moments which occur due to variation in the location of the radial thrust vector will be small. In view of this, it was decided to discontinue making moment measurements.

A set of circumferential pressure taps at each of five axial locations along the inside surface of nozzle No.1 enabled the pressure to be measured during operation. Measure--menta were made for both the port closed and port open modes of operation. The pressure coefficient K_p was computed and plotted versus angular position with respect to the control port for each normalized axial location Z/L. The plots for the port closed and port open cases are shown in Figs.11 and 12 respectively. The port is located at an axial postion Z/L of .39 to .45. The axial location of the propeller is such that the trailing edge of the propeller is flush with the leading edge of the port. It is apparent from Fig.11, in which the

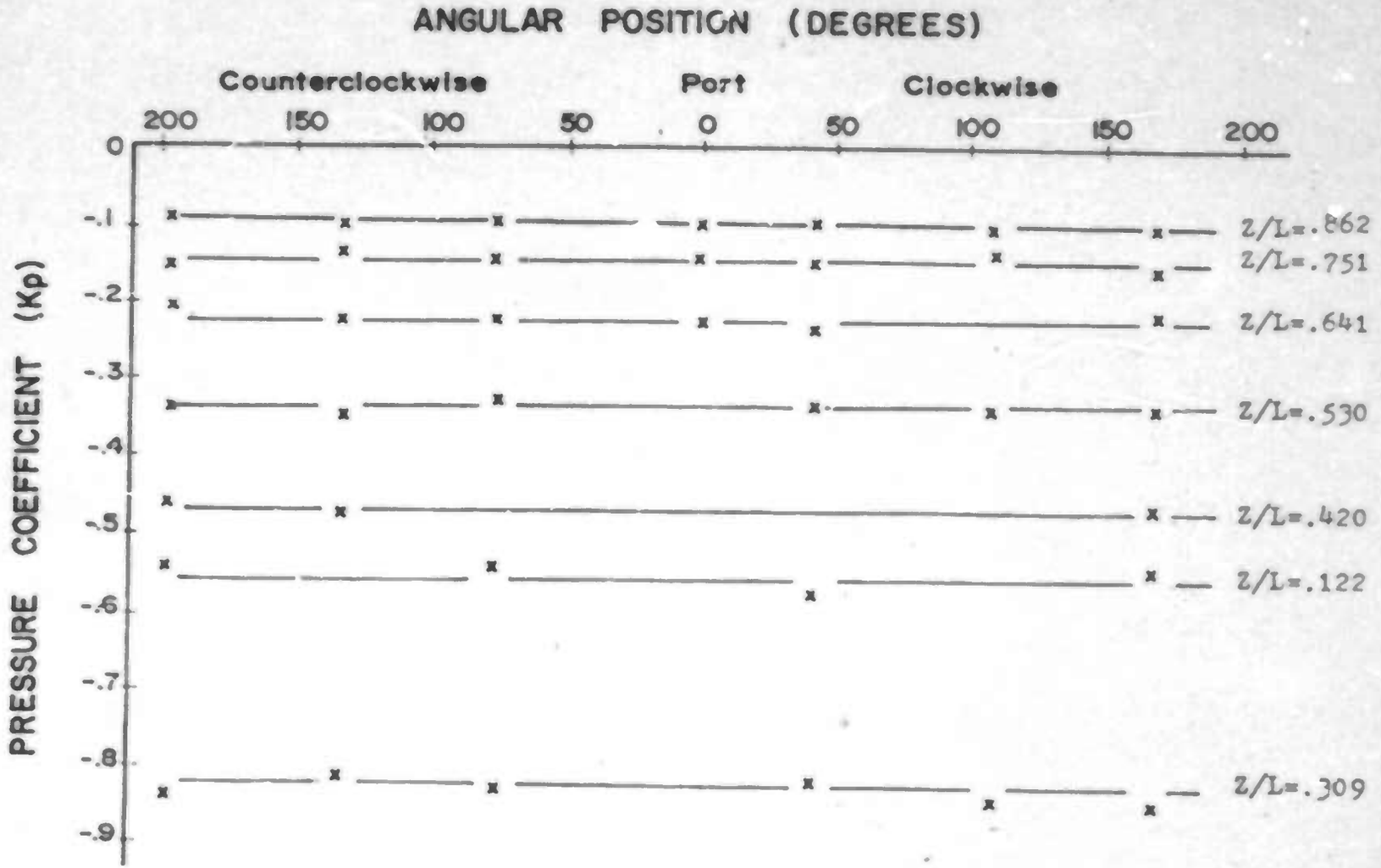

Fig.11 Closed Port Pressure Distribution for Nozzle No.2

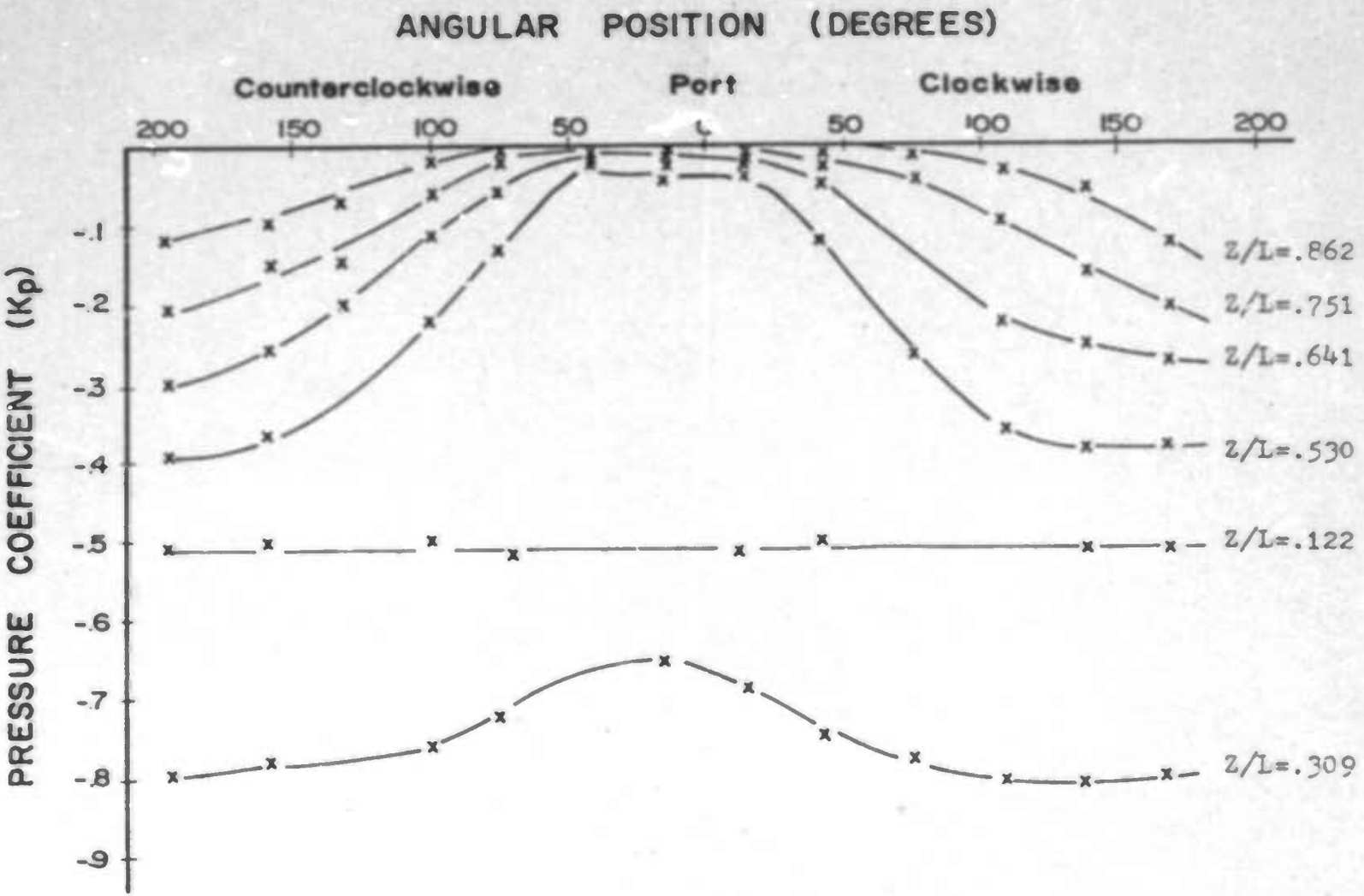

Fig.12 Open Port Pressure Distribution for Nozzle No.2

values of K_p at each axial location do not change with angular position, that the wake flow is symmetric with respect to the propeller axis. Thus, no radial force is being produced. Open--ing the port results in separation of the wake downstream of the port, producing a radial thrust in the approximate direction of the port. This is evident by comparatively higher (near zero) values of K_p in Fig.12. Note that the pressures ahead of the propeller plane ($Z/L = .12$) and in the vicinity of the prop--eller plane ($Z/L = .31$) are not appreciably affected. The slight antisymmetrical distribution in the pressure coefficient about the port in Fig.12 is attributed to the rotational motion imparted to the fluid by the propeller. This accounts for the measured rotation of the radial thrust vector for nozzles No.1 and No.2 given in Table 3.

From the data on WSN No.1 and No.2 in Table 3, nozzle No.1 appears to be the best choice as a propulsion-steering device since it has an appreciably higher steering ratio while producing almost the same axial thrust. However, there is another important factor to be taken into consideration.

Observation of separation and reattachment of the wake from inside nozzle No.1 and No.2 revealed an inconsistency in the behavior pattern of the wake. The wake from nozzle No.2 remained attached to the inside surface except when a port was opened,at which time it would switch, producing a radial force.

The wake would reattach when the port was closed. Nozzle No.1 followed the same pattern except that the wake would not re--attach after the port was closed. Instead, the wake from nozzle No.1 would remain separated and oscillate in an erratic manner and would not reattac unless the propeller speed was reduced. This necessitated a means for interpreting the reliabilty of a WSN.

To be reliable, a WSN must develop a radial force only with a control port open. This force must disappear when the port is closed. Allowances are made for the transition time or time for the flow field to re-establish after a port has been opened then closed. A WSN is defined as reliable if the transition time is less than 3 seconds, marginally reliable if it is greater than 3 seconds but less than 15 seconds and un--reliable if the time is greater than 15 seconds or if the wake separates when the port is not opened.

It should also be pointed out that some circumfer--ential separation of the flow at the trailing edge of both nozzles was observed using flow visualization techniques. This separation was much more pronounced in nozzle No.1 than for nozzle No.2. In preliminary tests on nozzle A3, a long stream--lined hub was added. It was found that the addition of this hub created or promoted separation of the flow at the trailing edge to the point where the shroud operated unreliably. The data

from these tests is contained in Appendix 1. Two models were sketched from observations of the flow field using air bubbles and streamers entrained in the flow. Figs. 13(a) and 13(b) depict the flow field of a WSN without the hub and with the hub, respectively. One plausible explanation for this behavior is that the hub provides a smooth continuous surface for the flow near the propeller axis to follow. Thus the fluid velocity with the hub is greater along the propeller axis and lower along the shroud surface. The resulting lower momentum of the fluid at the shroud surface causes separation to occur earlier in the flow. It was also observed for some nozzles that incr--easing vibration by removing the dampers improved nozzle reliability.[12,14]

2.4 Analytical Modelling of the Nozzle Flow Field

The experimental work in the previous section gives some indication of the complexity of the flow field of the WSN. To assist us in our investigation of the WSN, the development of a mathematical model capable of describing the flow field of the WSN was considered.

The problem of mathematically modelling the flow field in and around conventional shrouded or nozzled propellers is difficult. Some hydrodynamic models have been developed but in spite of their sophistication, agreement with the test results

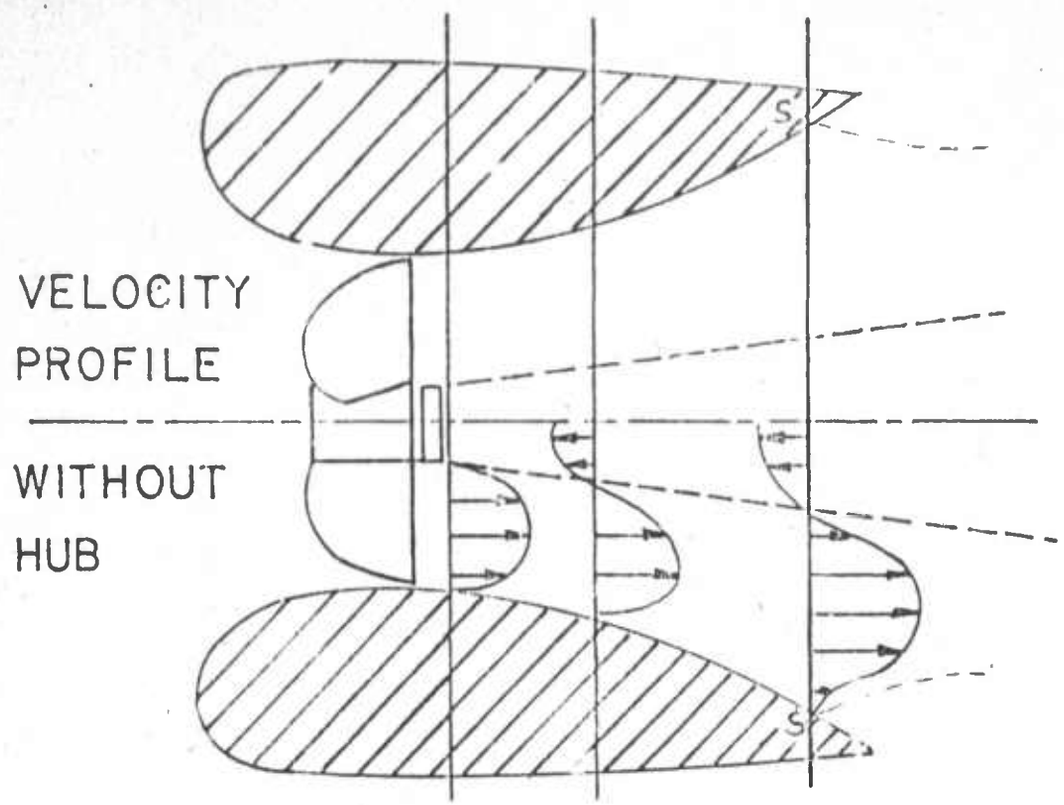

a) Without Propeller Hub

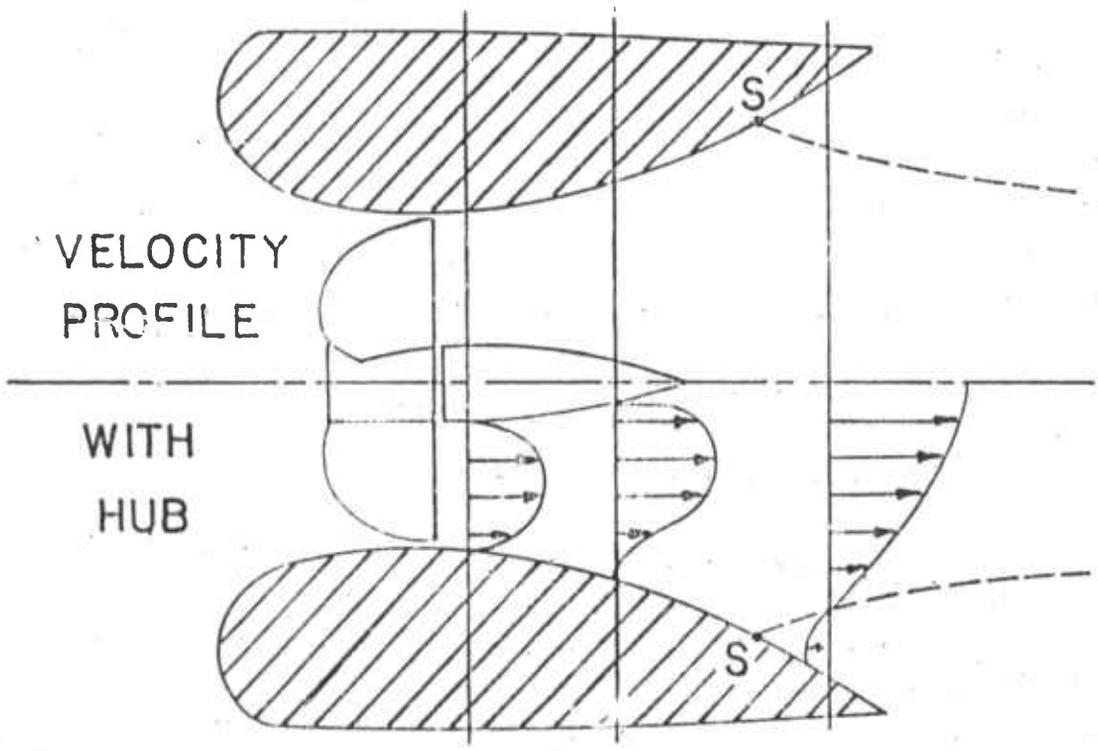

b) With Propeller Hub

Fig.13 Flow Field of the Wake Steering Nozzle

over a range of operating conditions has only been fair.[6-8] In addition, these models are valid only for axisymmetric flows and therefore apply only to the port closed case. Still, the possibility of using these analyses to predict the pressure distribution along the inside nozzle surface was considered. By designing the nozzle shape aft of the propeller plane to have as negative a pressure distribution as possible, it was felt that a maximum radial thrust could be produced. According to Fig.12, the pressure downstream of the port is essentially ambient for the open port case, thus, by making the pressure distribution as negative as possible, a large radial thrust should result when the control port is opened.

In axisymmetric hydrodynamic models developed in the literature, the approach used is to model the flow by means of a distribution of ring vortices and ring sources.[6-8] Most of these models are based on linear theory which means the ring vortices and sources lie along a cylinder and the model is only valid for shroud shapes which do not deviate greatly from a cylindrical shape. It is also assumed that the flow does not separate from the nozzle.

The preceeding two assumptions limit the applica-bility of the models since most of the shrouds investigated herein deviate substantially from a cylindrical shape and exibit some separation along the trailing edge. Aside from

these considerations the utility of the pressure predictions for the closed port case as a means of maximizing the radial thrust is questionable. This is apparent from the pressure plots in Fig.14.

Fig.14 is a plot of the pressure coefficients as a function of axial location for nozzles No.1 and No.2 with all ports closed. Since the pressure distribution is axisymmetric, the pressure coefficient is a function of axial location alone. Comparing the two profiles, it is not obvious that the open port radial thrust of nozzle No.1 would be about 40% greater than for nozzle No.2 as indicated in Table 3. The length of the shroud aft of the propeller plane is almost the same for each nozzle: 5.65 cm. for No.1 versus 5.23 cm. for No.2. The magni--tude of the pressures in the vicinty of the ports is almost the same while the pressure downstream of the ports is even more negative for nozzle No.2 than for No.1, leading one to believe that No.2 would produce a greater radial thrust. Thus, the port closed pressure distribution is of little use in predicting WSN radial thrust.

It would appear then, that to be of any real benefit, the mathematical model used must be capable of modelling the flow field with the port open. Because of the immense mathe--matical difficulties posed by the non-symmetric and separated nature of such a flow field, both within and around the outside

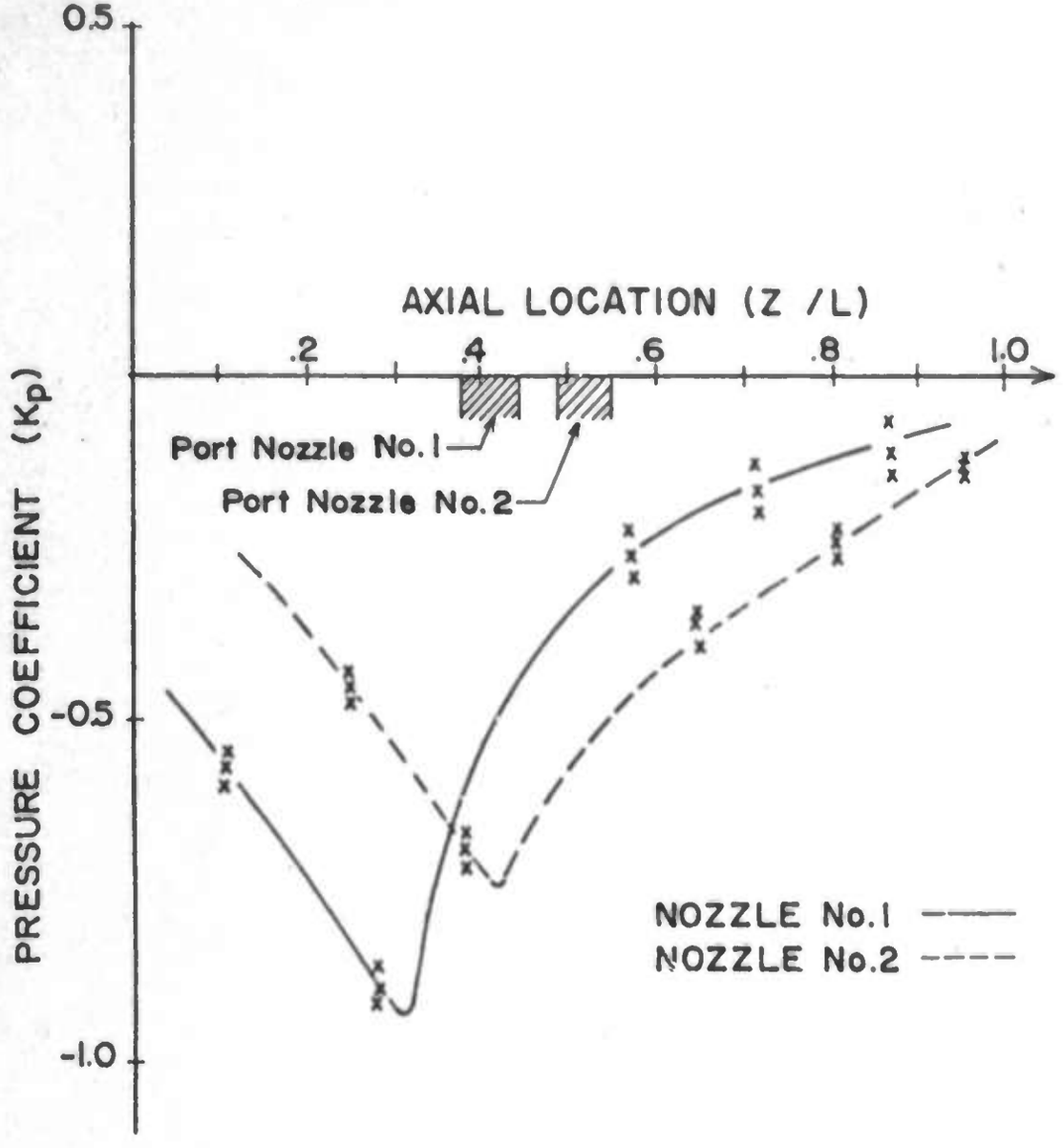

Fig.14 Port Closed Axial Pressure Distribution for Nozzles No.1 and No.2 with Propeller No.2

of a shroud operating in this mode, it was felt that a useful hydrodynamic model was not within the scope of this project based on the resources and time available. It was therefore decided to concentrate our efforts on experimentally evaluat--ing and developing the wake steering nozzle. Certainly, if the concept proves feasible and highly applicable, then one of the next steps should invclve both extensive theoretical and exper--imental work.

2.5 Experimental Investigation Of Major Parameters

The preliminary tests revealed that to develop a high radial thrust requires shrouds of comparatively high divergence. However, separation and thus reliability becomes a problem with the more divergent shrouds. Clearly a trade--off exists between the two conflicting divergence require--ments of small divergence for no separation and large diverg--ence for useful deflection of the flow in the steering mode. It was our objective in this set of tests to determine this trade-off and how it is affected by propeller pitch and nozzle length. Previous researchers, principally Van Manen,[4,5] have shown propeller type and nozzle length to be highly signifi--cant factors affecting nozzle-propeller performance.

The arc of a circle was chosen to describe the nozzle aft section. The cicle was chosen because it is easier

to standardize than for example a parabola. Also it turns out that the arc of a circle is a good approximation for the inside surface of nozzle No.1 and No.2 tested previously. The diver--gence angle of the nozzles was then varied by simply varying the radius of curvature R_c shown in Fig.8. This generated nozzle series A. Nozzle series B was generated by cutting the most divergent shroud in nozzle series A to various lengths to generate the same divergence angles as series A. These two series, described in Table 2, were tested over the complete range of propeller pitch given in Table 1. The data from these tests is presented in Table 4 and Table 5.

The values of K_{TA} in Tables 4 and 5 are based on the axial thrust measured with the port closed and the wake flow symmetrical such that no radial thrust is produced. The absence of measurements of K_{TA} in the tables indicates that this state did not exist. A small decrease between the port open and port closed values of K_{TA} was observed for nozzles which were re--liable and marginally reliable (1-5%). For unreliable nozzles where the wake failed to reattach when the port was closed K_{TA} increased slightly.[12,14]

TABLE 4

EFFECTS OF MAJOR PARAMETERS ON NOZZLE PERFORMANCE CHARACTERISTICS - SERIES A

Nozzle	R_c/D	L_a/D	P/D	K_{TA}	K_{TR}	$K_{TR/A}$	θ_r	Rel*
A1	5.28	1.14	1.24	.417	.053	.127	40.5	R
			1.41	.614	.104	.169	44.9	R
			1.64	.607	.067	.110	47.4	R
			1.73	.807	.092	.114	55.2	R
			1.97	.942	.098	.104	57.0	R
			2.06	.907	.080	.088	61.3	R
A2	3.43		1.24	.380	.070	-	33.8	U
			1.41	.578	.138	.239	37.5	R
			1.64	.566	.133	.235	40.4	R
			1.73	.751	.175	.233	42.4	R
			1.97	.891	.177	.199	55.1	R
			2.06	-	.192	-	48.0	U
A3	2.93		1.24	.352	.101	-	35.5	U
			1.41	.542	.186	.343	35.8	R
			1.64	.498	.168	.337	47.0	M
			1.73	.713	.228	.320	34.7	R
			1.97	.833	.216	-	48.1	U
			2.06	-	.214	-	50.4	U
A4	2.43		1.24	.339	.128	-	33.0	U
			1.41	.518	.193	.373	31.8	M
			1.64	.524	.204	.389	34.6	M
			1.73	.670	.242	.361	34.5	M
			1.97	.733	.236	-	41.1	U
			2.06	-	.247	-	45.9	U
A5	2.19		1.24	.326	.152	-	27.8	U
			1.41	.492	.243	.494	30.7	M
			1.64	.479	.241	.503	33.6	M
			1.73	.619	.312	.504	36.2	R
			1.97	.735	.332	-	41.0	U
			2.06	-	.305	-	42.3	U

*Reliability: R = reliable, M = marginally reliable, U = unreliable

TABLE 5

EFFECTS OF MAJOR PARAMETERS ON NOZZLE PERFORMANCE CHARACTERISTICS - SERIES B

Nozzle	$R_{c/D}$	$L_{a/D}$	P/D	K_{TA}	K_{TR}	$K_{TR/A}$	θ_r	Rel*
B1	2.19	0.47	1.24	-	.035	-	27.6	U
			1.41	-	.051	-	28.3	U
			1.64	-	.054	-	26.9	U
			1.73	-	.059	-	27.8	U
			1.97	-	.082	-	33.4	U
			2.06	-	.079	-	33.7	U
B2		0.72	1.24	-	.102	-	25.9	U
			1.41	-	.112	-	27.0	U
			1.64	-	.168	-	29.8	U
			1.73	-	.211	-	31.5	U
			1.97	-	.259	-	32.7	U
			2.06	-	.223	-	36.6	U
B3		0.85	1.24	-	.130	-	28.2	U
			1.41	.599	.183	-	28.0	U
			1.64	.609	.207	-	29.8	U
			1.73	.702	.224	-	31.5	U
			1.97	-	.307	-	32.8	U
			2.06	-	.256	-	36.4	U
B4		1.02	1.24	.351	.144	-	26.5	U
			1.41	.521	.194	.372	31.2	M
			1.64	.524	.216	-	34.1	U
			1.73	.678	.263	.388	35.9	M
			1.97	.802	.307	-	37.6	U
			2.06	-	.274	-	36.7	U
B5		1.14	1.24	.326	.152	-	27.8	U
			1.41	.492	.243	.494	30.7	M
			1.64	.479	.241	.503	33.6	M
			1.73	.619	.312	.504	36.2	R
			1.97	.735	.332	-	41.0	U
			2.06	-	.305	-	42.3	U

*Reliability: R = reliable, M = marginally reliable, U = unreliable

The data in Tables 4 and 5 reveal some general trends:

Axial thrust
- decreases with nozzle divergence.
- decreases with nozzle length.
- increases with propeller pitch to diameter.

Radial thrust
- increases with nozzle divergence.
- increases with nozzle length.
- exhibits a slight maximum when plotted against propoller to diameter ratio.

Steering ratio
- increases with nozzle divergence.
- remains almost constant with propeller pitch to diameter.

Thrust angle
- decreases slightly with nozzle divergence.
- remains almost constant with nozzle length.
- increases with propeller pitch to diameter ratio.

Reliability
- decreases with nozzle divergence.
- increases with nozzle length.
- appears greatest for propellers which are "mid-range" in terms of pitch to diameter ratio.

2.6 Summary and Conclusions

The performance of the WSN at zero forward velocity was investigated. The preliminary tests revealed that the radial thrust of the WSN could be increased by increasing nozzle divergence. However, higher nozzle divergence resulted in an unreliable mode of operation where the wake remains de--flected after closing the control port, producing an erratic radial thrust.

A further set of tests were conducted varying nozzle divergence and length and propeller pitch to diameter ratio to determine their effects on the thrusting and steer--ing characteristics of the nozzle. A number of propeller--nozzle combinations were found which exhibited reliable or marginally reliable operation.

This set of shrouds is almost exclusively confined to the longer nozzles of series A. Nozzle A1 was the most reliable over all, as it worked well with all the combinations of propellers. However, for use as a steering device, it is the least desirable since it also produces the smallest steer--ing ratio. According to the combined criteria of large steer--ing ratio and reliable operation, nozzle A5 is the optimum choice.

The best propeller to use would appear to be propeller

No.4 with P/D = 1.73 which operated the most reliably. It should be pointed out that the reliability of all the prop--ellers was sensitive to the axial location of the propeller with the optimum location of the propeller being at the point where the trailing edge of the propeller was flush with the leading edge of the port. Propeller location became more critical as nozzle divergence was increased. Propellers No.2 and 3 also performed reasonably well. Propeller No.3 operated somewhat less reliably than No.2 and also produced a lower axial thrust. This could be due to the smaller diameter and therefore larger tip clearance of propeller No.3 (D = 4.32 cm. vs 4.42 cm.). Too large a tip clearance enables backflow around the tips of the propeller blades lowering propeller efficiency.(4)

The static tests have demonstrated that the concept is feasible, but much more information is required to enable an assessment of the potential of the WSN as a submersible propulsion-steering device. Most important is the effect of forward velocity on reliability and steering ratio. In addition, forward velocity data would enable the propulsion efficiency of the WSN to be compared to more conventional nozzled propellers.

3. FORWARD VELOCITY TESTING OF THE WAKE STEERING NOZZLE

The previous section dealt with the experimental investigation of the static performance of the WSN. One of the prime requirements in evaluating any propulsion-steering system for marine vessels is a knowledge of its behavior over a range of forward velocities. This is also true for rescue submersibles where the typical rescue mission calls for a rapid transport leg between the mother ship and the site of the distressed submarine.

This section is concerned with evaluating the effect of forward velocity on the performance characteristics of the WSN identified in Section 2, particularly the radial steering force, nozzle reliability and an additional performance parameter, the efficiency of the WSN as a thruster. Two nozzles from the static tests, nozzles A2 and A3, were chosen for evaluation with a number of propeller types over a range of forward velocities. These nozzles were chosen because they were about "mid-range" in terms of reliability and steering force in the static tests, thus enabling a shift in either direction in their performance characteristics to be detected. A forward velocity tunnel and measurement system were designed and constructed to enable these tests to be carried out. The shrouds used were manufactured out of aluminum and streamlined to reduce the fluid drag forces. Some preliminary tests were also conducted to

investigate controlling the wake separation to produce a pro--portionally controlled steering force by locating several ports axially along the shroud surface downstream of the propeller.

3.1 Forward Velocity Test Facility

To simulate forward velocity, a water tunnel was designed and constructed by Hudson and Wilson.[15] The tunnel consisted of an open channel (.61 m high x .31 m wide). For a water depth of .31 m, the system is capable of producing water velocities of up to 1.22 m/sec. based on a maximum pump capacity of 7580 litres/min. Water enters the channel, shown in Fig. 15, through a pipe. To minimize entrance effects and straighten the flow downstream, a short section at the begin--ning was fitted with screens and a honeycomb mesh of small tubing. Preliminary testing of the water tunnel revealed that the axial flow velocity downstream of this section is nearly uniform, varying at most $\pm$ 5% across the channel, except at points very near the channel walls and water surface.[15] The sides of the channel were constructed out of plexiglass to enable the use of flow visualization techniques.

The nozzles tested were constructed out of aluminum and the outside surface streamlined to minimize drag and inhibit flow separation. Fig.16 shows the basic WSN configuration used

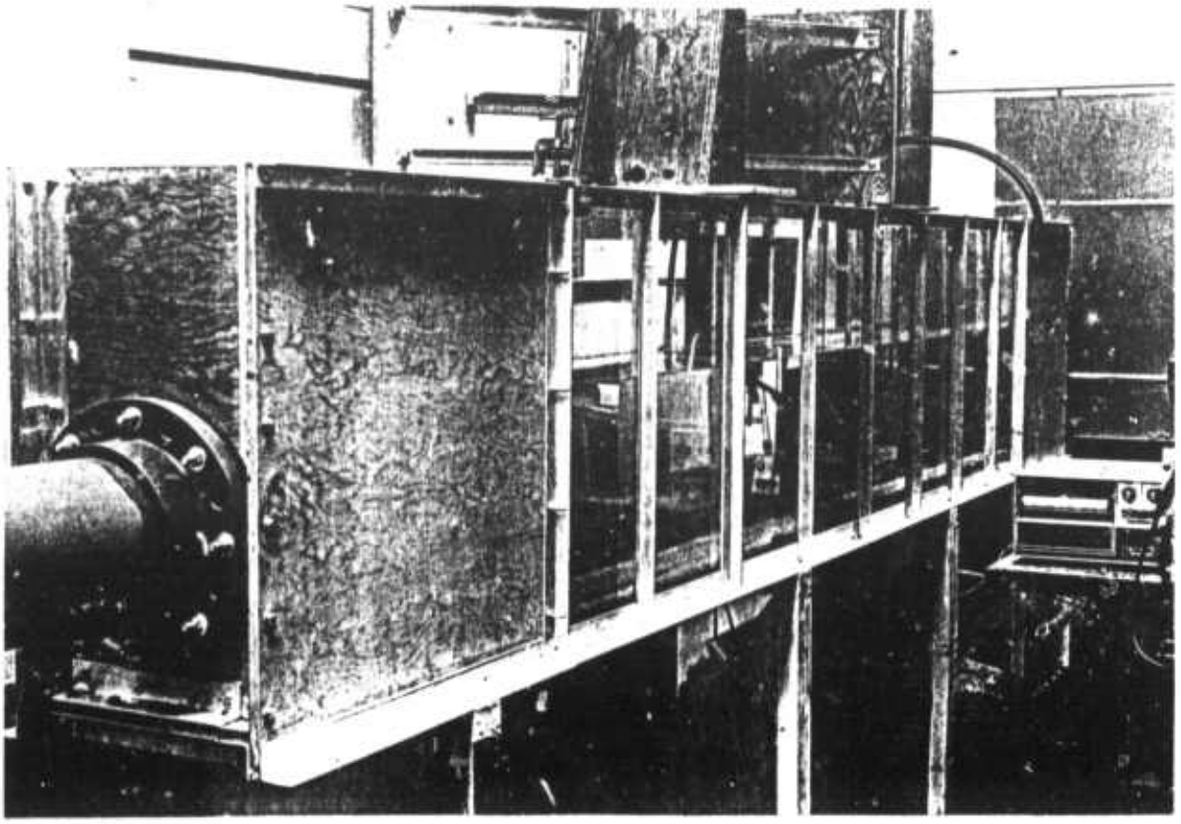

Fig.15 Water Channel Used for Testing Forward Velocity Nozzles

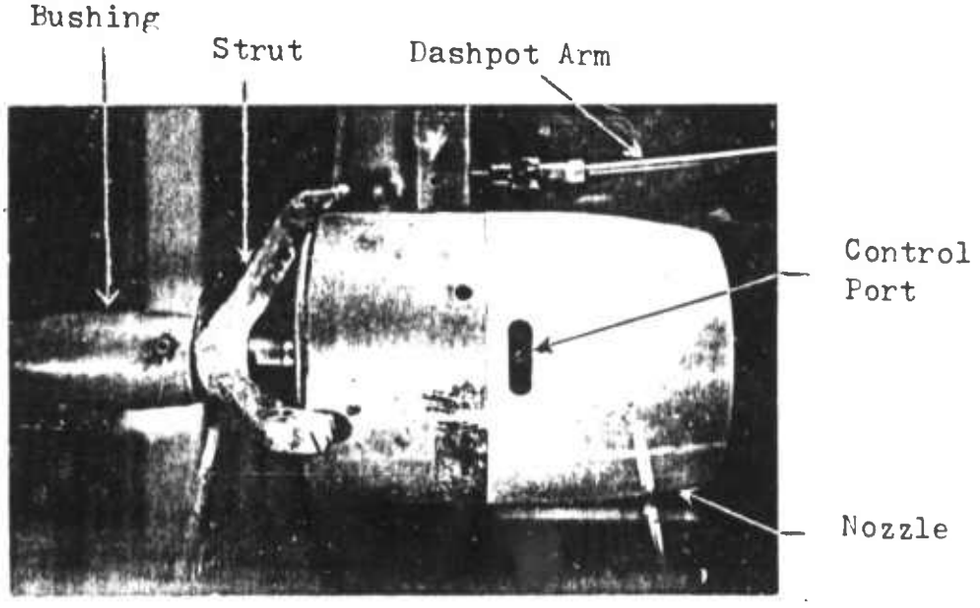

Fig.16 The Basic Configuration of the Wake Steering Nozzles Used for the Forward Velocity Tests

in forward velocity tests. Three nozzles were constructed having the same inside shapes as nozzles A2, A3 and A4 used in the static tests. Since the front section of these nozzles is the same for all three, only aft sections varied. This was accomplished by providing a tongue and groove type of fitting between the front and aft sections enabling the aft sections to be easily changed and providing a smooth surface between the two sections. The front section of the test nozzle is shown to full scale in Fig. 17(a). The outside surface of the nozzle is cylindrical except for the last 5.1 cm of the aft section which was streamlined by making it converge. The convergence of the outside surface is described by the arc of a circle as indicated in the schematic of Fig. 17(b). The numerical values for the geometric parameters describing the nozzle aft sections are given in Table 6.

The radial and axial thrust, motor speed and pro--peller torque were measured using the same basic system as in the static tests except a streamlined strut was added to the dynamometer to reduce the drag. The propeller bushings and struts were also streamlined.

Nozzle A3 with propeller No.2 is shown in operation with all the ports closed in Fig. 18(a). Air bubbles injected upstream of the nozzle show that the wake flow is symmetrical

about the propeller axis. Fig.18(b) shows the degree of wake deflection when a port near the top of the shroud is opened.

TABLE 6

AFT SECTION SHAPES OF NOZZLES FOR FORWARD VELOCITY TESTING

Nozzles	$L_{a/D}$	$R_{c/D}$	$R_{co/D}$
A2	1.43	3.43	3.68
A3	1.43	2.93	4.72
A4	1.43	2.43	4.65

D = 4.45 cm.

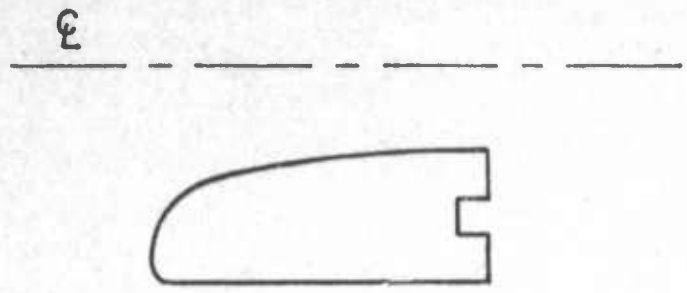

a) Front Section

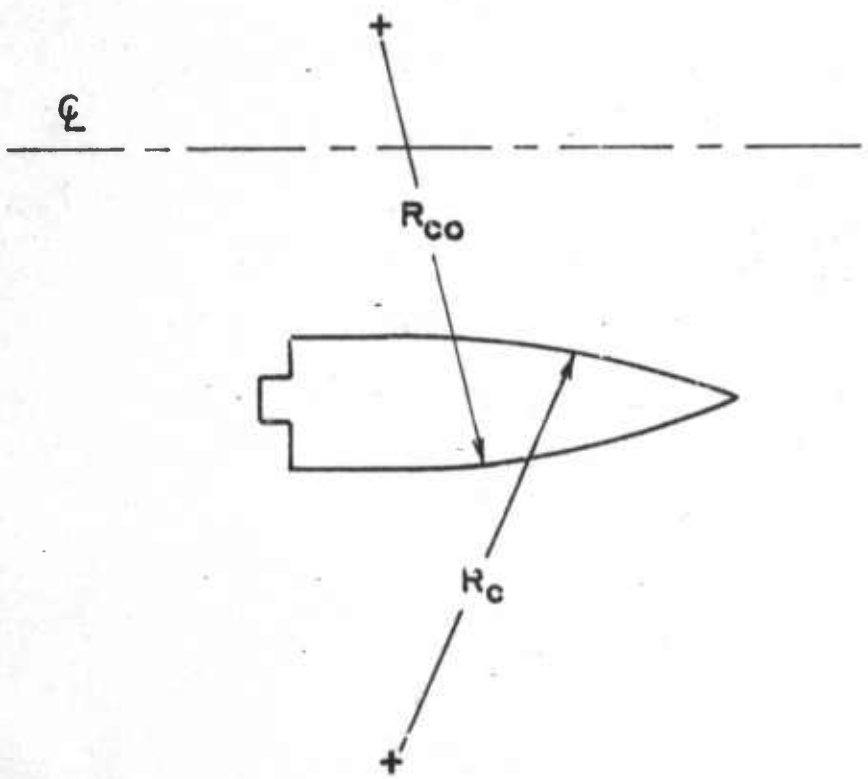

b) Aft Section

Fig.17 Geometric Parameters of the Forward Velocity Wake Steering Nozzles

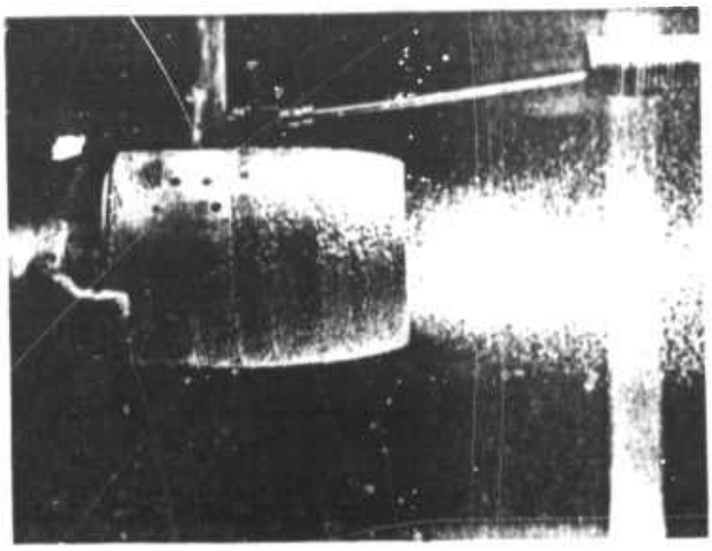

a) All Ports Closed

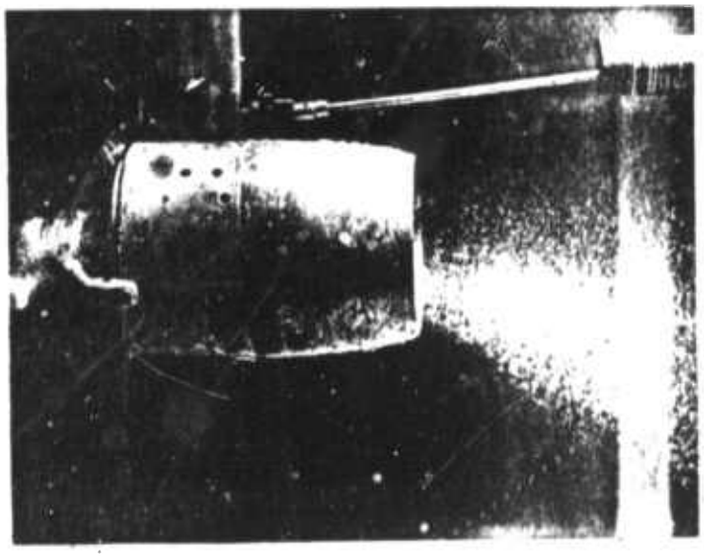

b) Top Port Open

Fig.18 Flow Pattern of Nozzle A3 with Propeller No.2

3.2 Effect of Forward Velocity on WSN Performance Characteristics

The previous described test facility was used to evaluate the performance of nozzles A2 and A3 over a range of fluid velocities. Nozzle A4 was used in the investigation of radial force control. A representative variety of propeller types were selected from those used in the static tests. The propellers used for the forward velocity testing were numbers 1,2,4 and 5 and are described in Table 1. These two shrouds were tested by Hudson over a range of motor speeds from 23.6 rev./sec. to 63.6 rev./sec. and at tunnel velocities of from .21 meters/sec. to .77 meters/sec. The results from the tests are represented in normalized form by plotting the axial thrust coefficient K_{TA}, radial thrust coefficient K_{TR} and efficiency η against the nondimensionalized velocity or advance coefficient J.[4]

Typical curves showing the spread of data points for one nozzle-propeller combination, nozzle A3 with propeller No.4, are shown in Fig.19. Figs.20 and 21 summarize the test results for the complete series of propellers tested with nozzles A2 and A3, respectively.

It should be pointed out that the values of axial thrust coefficient are based on the values of system thrust where the only drag force included is the drag of the shroud. In other words, the dynamometer and propeller struts and bushing

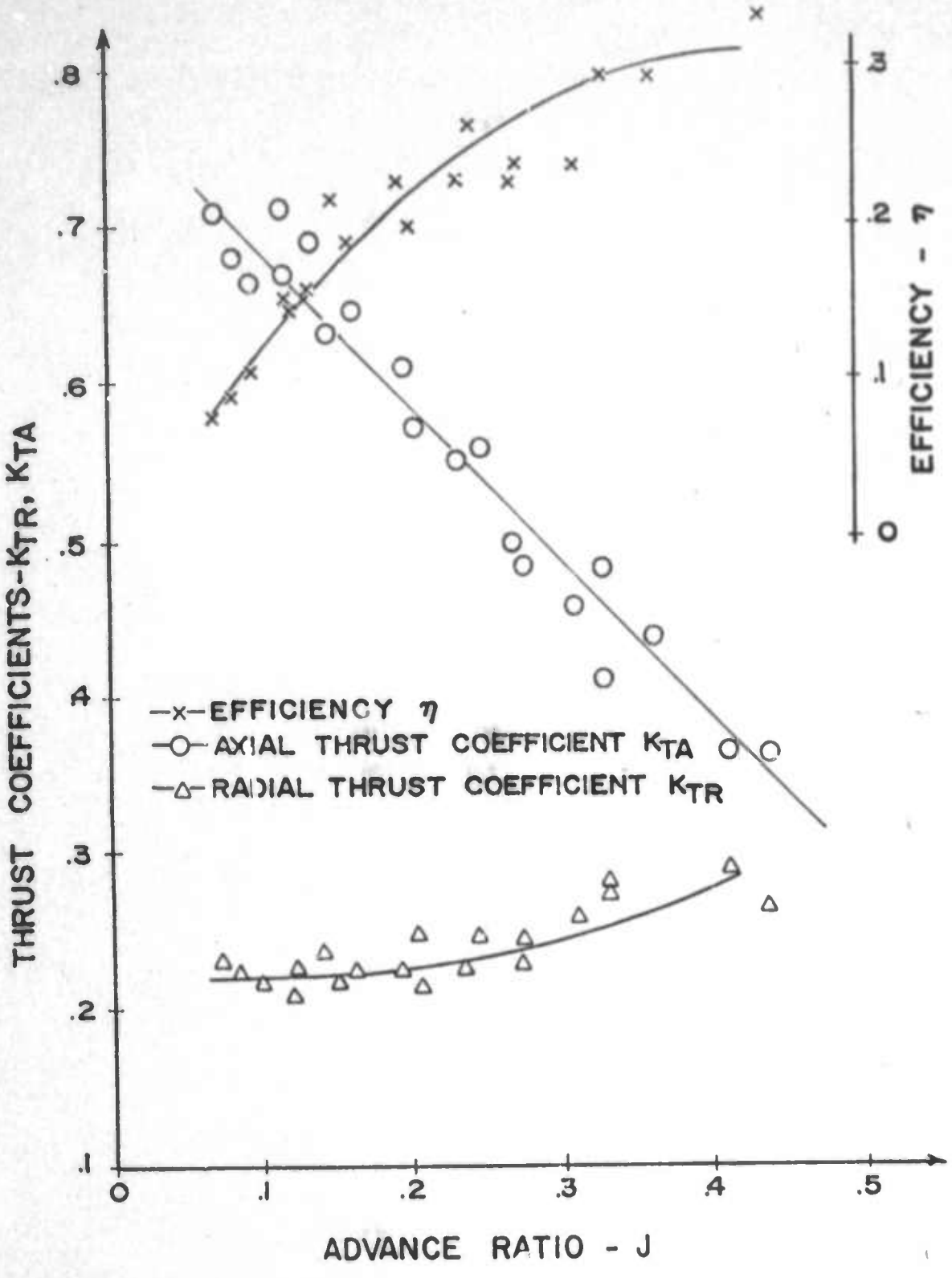

Fig.19 Forward Velocity Test Results for Nozzle A3 with Propeller No.4

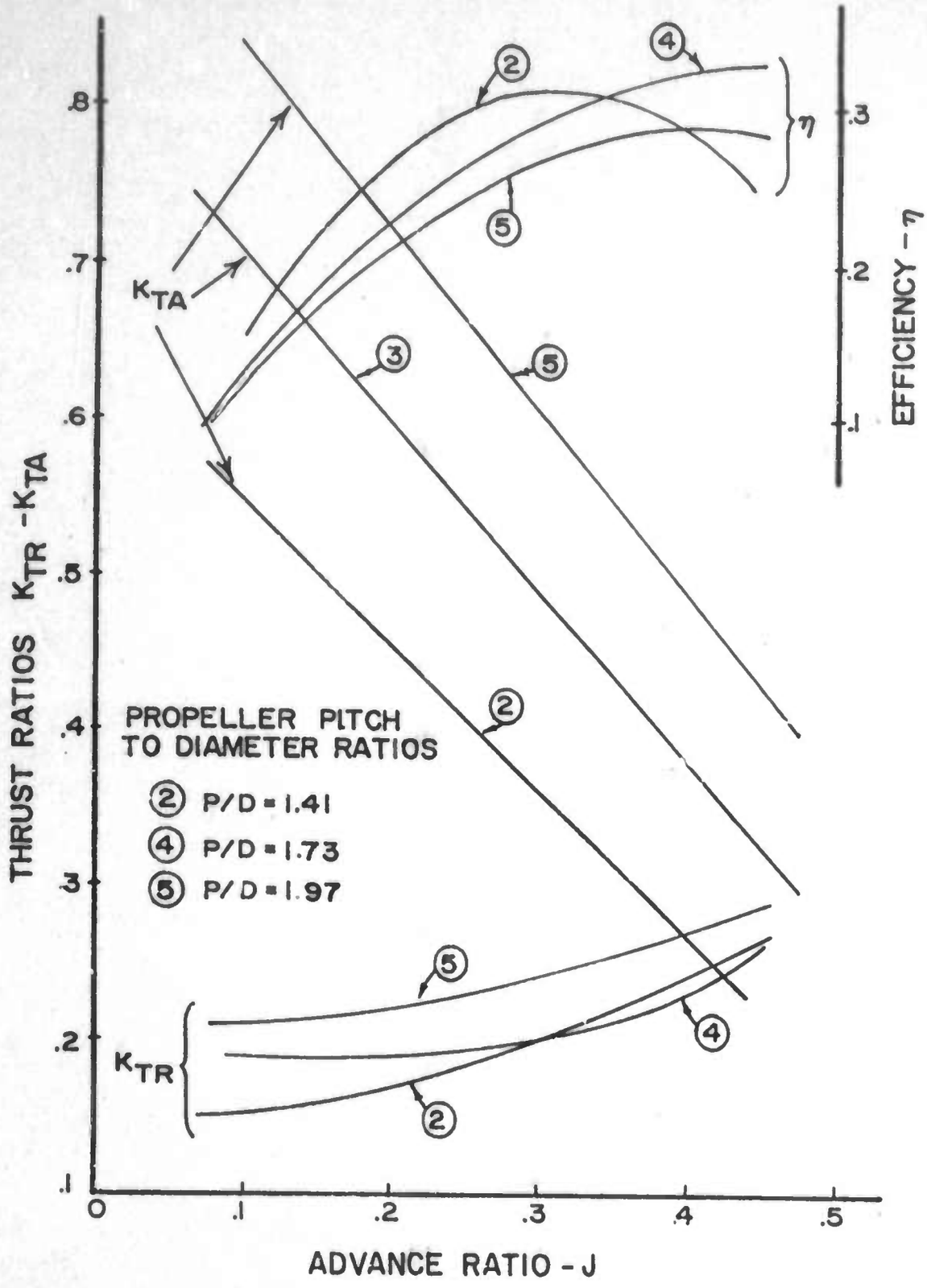

Fig.20 Forward Velocity Test Results for Nozzle A2 with Propellers No.2, 4, and 5

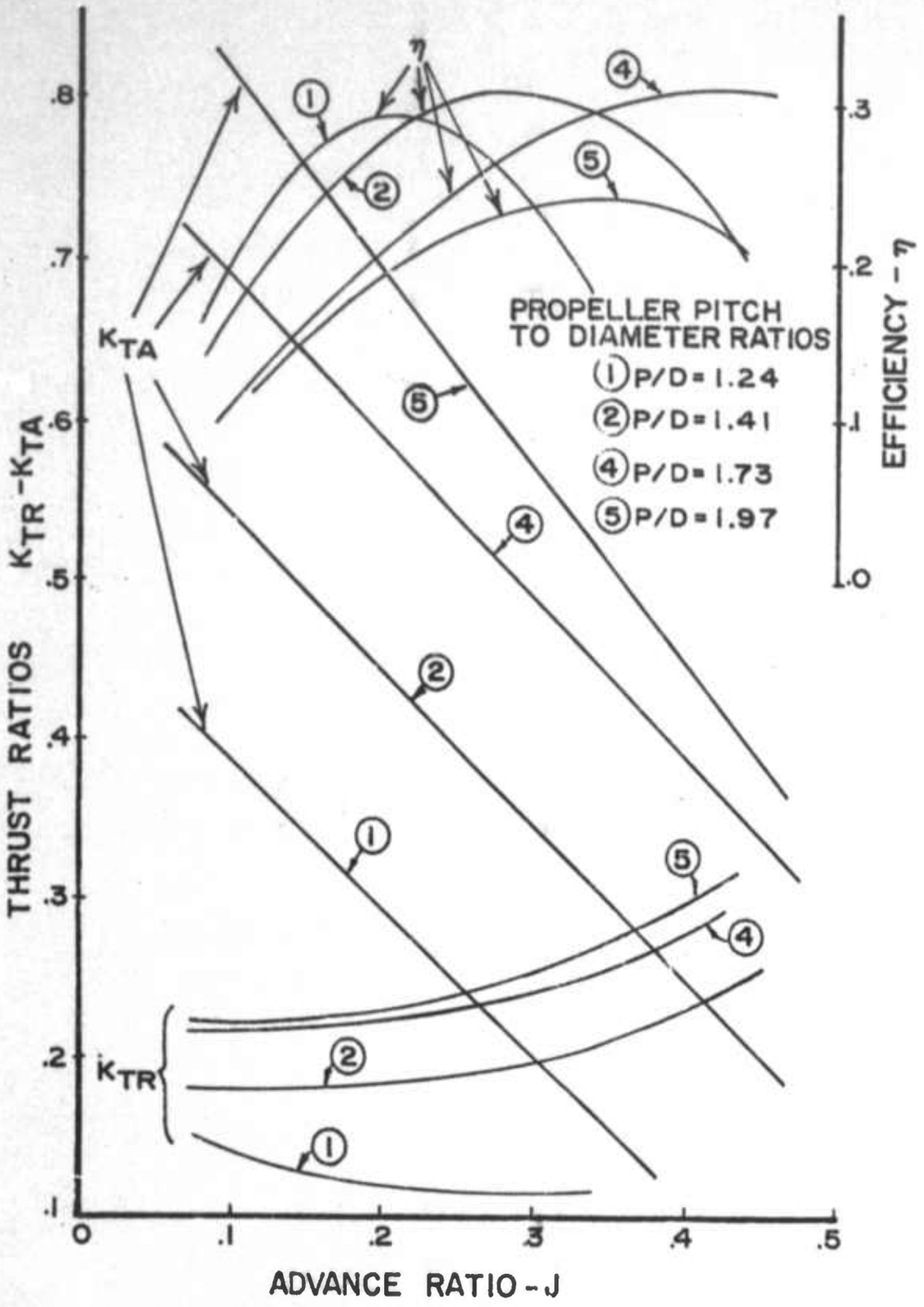

Fig.21 Forward Velocity Test Results for Nozzle A3 with Propellers No.1, 2, 4, and 5

are not considered part of the basic system and the drag of these components was subtracted from the axial force before calculating the axial thrust coefficient and WSN efficiency. This is the same approach used by Van Manen and other researchers in analyzing the performance of nozzled propellers.[3-5] No difference between the drag forces of the two nozzles could be detected.[15] The axial thrust coefficient decreases with velocity or advance ratio as would be expected from basic propeller theory.[16] The values of K_{TA} are based on thrust measured with the control port closed. Axial thrust was observed to increase slightly when a control port was opened. The increase was greatest for those shrouds which operated with a high degree of circumferential flow separation from the inside shroud surface at the trailing edge. Except for propeller No.4 operating in nozzles A2 and A3, all combinations showed some degree of circumferential separation with all ports closed.

The radial thrust generally exhibits an increase with forward velocity as evident in Fig.20 and 21. This increase could be due to the observed rudder-like characteristics of the WSN. Tests conducted over a range of forward velocities on a nozzle without a propeller showed that the nozzle developed a small radial thrust which increased with forward velocity.[15] This increase is due to the fact that when a control port was opened the flow through the shroud became assymetric causing a radial thrust on the shroud even with no propeller.

The only propeller-nozzle which did not show an

increase in radial thrust with advance ratio was propeller No.1 operating in nozzle A3. Flow visualization techniques revealed that this combination was operating with the flow almost fully separated from the inside surface with all ports closed. This was a much higher degree of circumferential separation than was observed for any of the other combinations. This could account for the drop in radial thrust since previous pressure measure--ments revealed that the pressures were higher for separated flow. The reduced pressures would act to reduce control port flow and thus wake deflection.

All of the propeller-nozzle combinations worked re--liably, that is they all produced a radial thrust only when the control port was open and this thrust disappeared in less than three seconds after closing the port. This improvement in reliability over the static tests could be due to two factors. The momentum of the fluid flowing along the outside surface of the shroud is directed along the propeller axis. This flow would tend to force the deflected wake to return to an axisymmetric flow after closing the port. Also some leakage was observed to be occurring through the closed port in the static tests which would tend to make nozzle operation less reliable.

Fig.22 is a plot of the steering ratio for nozzles A2 and A3. Taken by themselves, these curves can be somewhat misleading since they would favor operation at a high advance

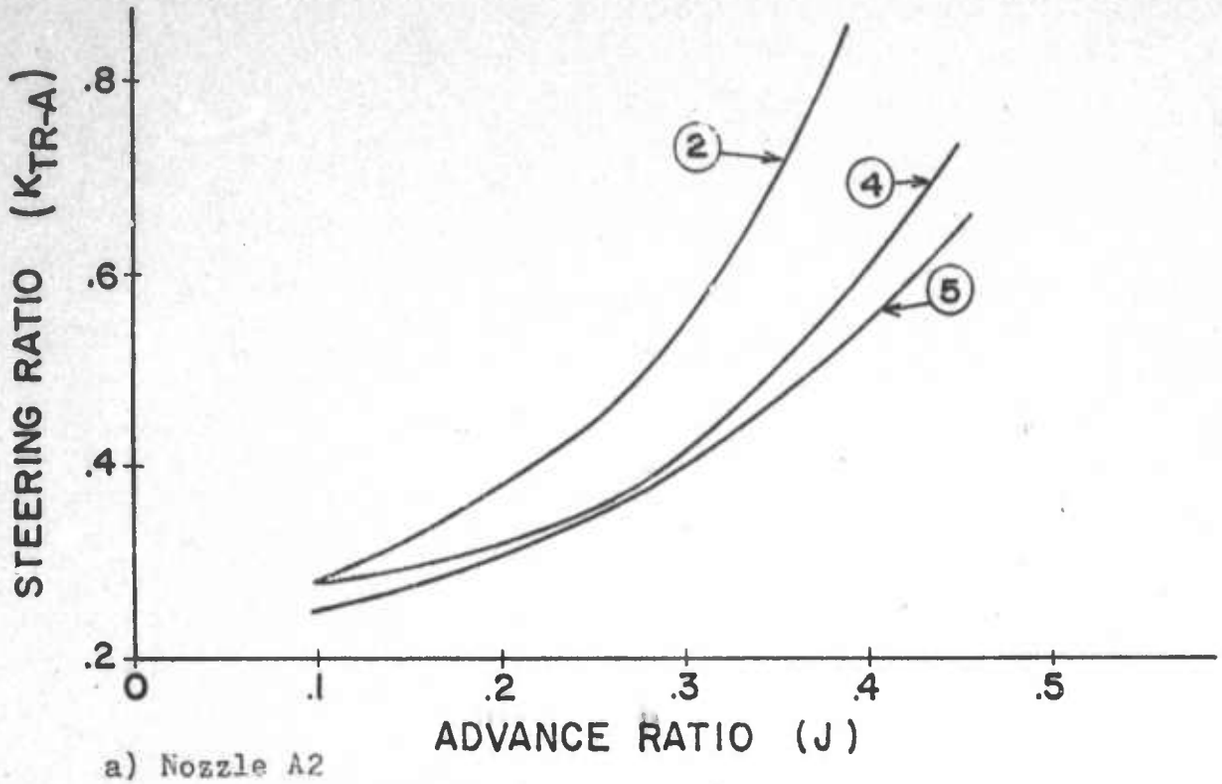

a) Nozzle A2

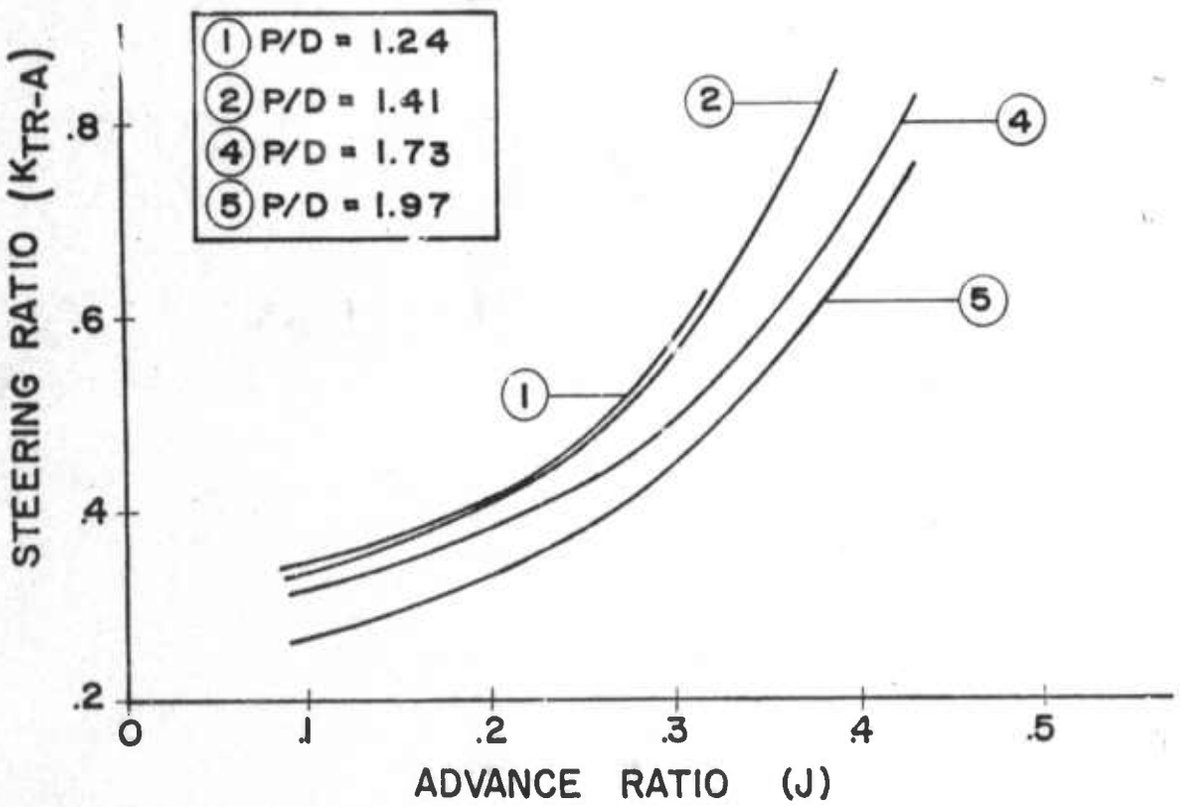

b) Nozzle A3

Fig.22 Steering Ratio Versus Advance Ratio for Nozzles A2 and A3

ratio and using propeller No.2. There are other considerations such as efficiency. Propellers No.2 and No.4 are the most effi--cient as indicated by Figs.20 and 21. From an efficiency stand--point, the choice between propeller No.2 and No.3 would depend on the advance ratio at which the vessel cruises. These aspects of propeller-nozzle selection from the design curves will be covered in more detail in the next section.

3.3 Radial Force Control: Preliminary Tests

The tests so far have demonstrated that a number of reliable propeller-nozzle combinations exist which develop radial thrusts of a reasonable magnitude. However, for a given control port this radial steering force is single valued, changing only with motor speed. To compete with other steering systems, the WSN should be capable of developing a steering force for which the magnitude can be controlled at any speed. As a result, a preliminary series of tests were conducted on nozzle A4 to inves--tigate a method of controlling the magnitude of the radial force.*

A series of ports were placed along the shroud, from just aft of the propeller plane up to the exit plane. It was felt that the magnitude of the radial force could be varied by varying the location at which a control port was opened, based

* This investigation was conducted by Mr. R. Gauthier as part of an Engineering Undergraduate Projects Course at the University of New Hampshire

on the assumption that a port near the exit plane would deflect the wake a smaller amount than a port just aft of the propeller plane. To test this out, three slotted ports were drilled to the same dimensions as the ports used in the previous tests (.098 cm. x .295 cm.).

The nozzle was tested with propeller No.2 over a range of forward velocities. The results are given in Fig.23. As exp--ected, the radial force magnitude decreases with the distance of port location from the propeller plane. Thus, the technique has potential for providing at least some degree of control over the radial force magnitude. Precise control might be possible if a system were designed to provide a control flow at any axial location. Additional test work is required to study the effect of axial port location and shape on other propeller-nozzle combinations.

3.4 Summary

The results revealed that the reliability of the WSN performance at nonzero forward velocity was improved over the static tests. The radial thrust coefficient showed a favorable increase with advance ratio while the axial thrust decreases as is the cases with all shrouded propellers. A method was developed for controlling the radial force magnitude by locating a series

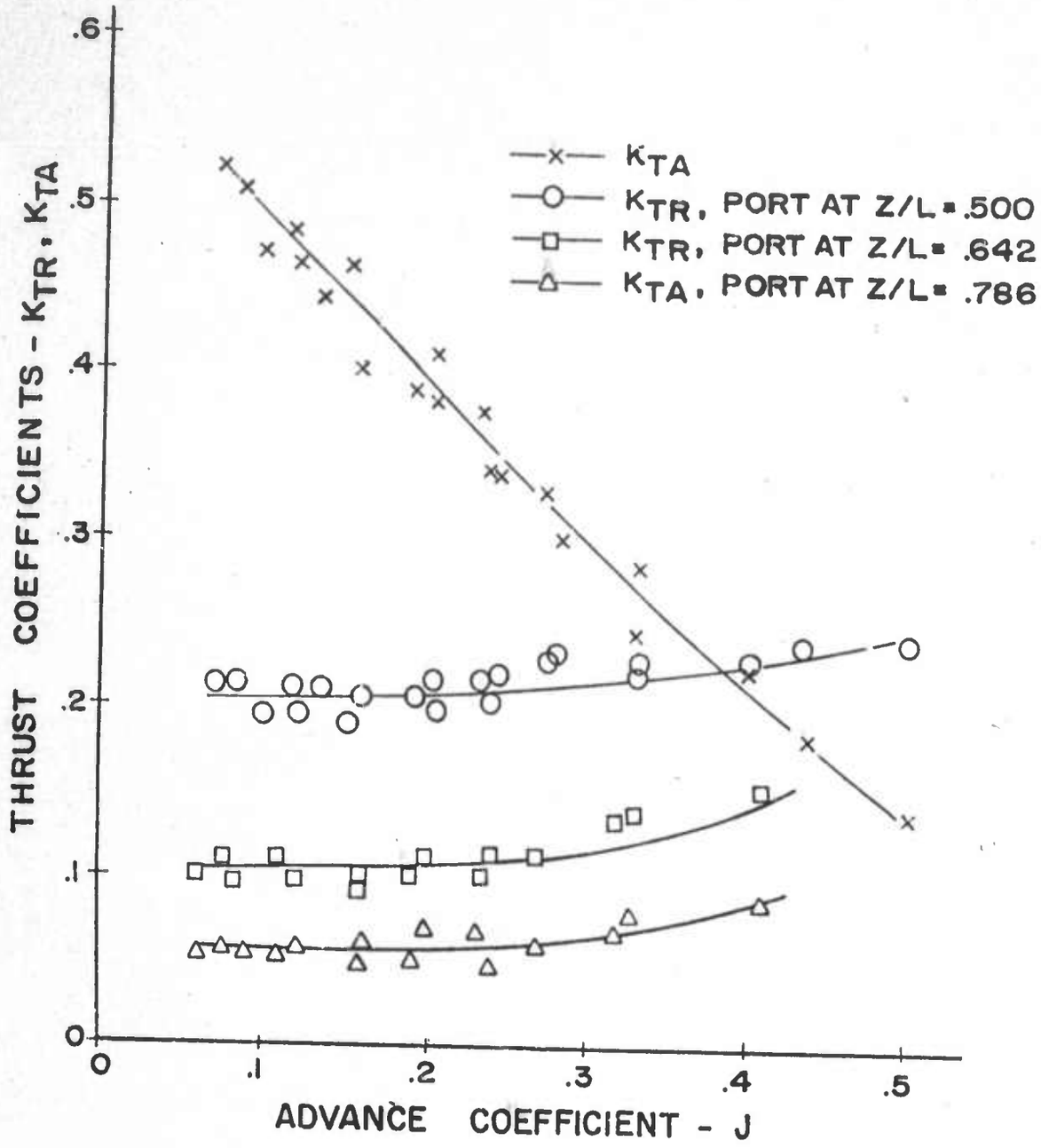

Fig.23 Effect on the Coefficient of Radial Thrust of Axial Location of the Control Port

of slots at different axial locations along the aft section of the shroud.

Additional test work is required to further extend the set of reliable propeller-nozzle combinations and to verify the method of radial force control for other WSN. Development work is also required to explore such factors as directional control of the radial force. However, before proceeding with more testwork an assessment of the potential of the WSN should be made. The combined static and forward velocity tests results have provided the necessary information. This can be accomplished by comparing the thrusting and steering characteristics to those of conventional submersible propulsion-steering systems.

4. AN EVALUATION OF THE PROPULSION-STEERING CHARACTERISTICS OF THE WAKE STEERING NOZZLE

The previous two sections have demonstrated the feasibility of the wake steering concept. Enough information on the operating characteristics of the WSN has been obtained to enable at least preliminary evaluation of the WSN as a propulsion-steering device.

In this section, the efficiency of the WSN as a thruster is evaluated by comparing the WSN efficiency to existing data for nozzled propellers.(3-5) The steering effect-iveness of the WSN is investigated for both the cruising or forward velocity mode and hovering mode. The steering effect-iveness during cruising is evaluated by comparing the WSN with a conventional submersible propulsion-steering device, a propeller surrounded by a tiltable shroud. The comparison is made by means of computer simulations of the submersible DSRV. This comparison is based on preliminary forward velocity tests on a model propeller and nozzle. The capability of the two WSN, one mounted fore and another aft as shown in Fig.3, to provide independent force and moment generation in the various degrees of freedom during hovering is discussed.

4.1 The Propulsive Efficiency of the WSN

Considerable experimental work on propellered nozzles has been conducted at the Netherlands Ship Model Basin (NSMB).[3-5] As a result of these efforts, a number of propellered nozzles have been developed which are highly efficient thrusters. Some of the test results showing the axial thrust coefficient and efficiency plotted as a function of advance ratio for one of the most efficient nozzles, nozzle 19a taken from Reference 24, Fig.22 are shown in Fig.24. This nozzle was tested with a series of four bladed propellers ranging in pitch to diameter P/D ratio from 0.6 to 1.6. The test results for two of the propellers having P/D ratios of 0.6 and 1.4 are shown in Fig.24 for comparison with one of the better performing wake steering nozzles tested at forward velocity, nozzle A3 with propeller No.2. The test results for 19a with propeller P/D ratio of 1.4 are used for comparison with the WSN because propeller No.2 has a nearly identical P/D ratio of 1.41. The results with the propeller P/D ratio of 0.6 were chosen because the peak efficiency of 19a with this propeller occurs at very nearly the same advance ratio as for the WSN.

One deficiency is apparent in comparing the WSN with nozzle 19a, the efficiency is lower. However, to a certain degree this is to be expected since nozzle 19a is a highly developed nozzle degign representing the state of the art in conventional nonsteering propellered nozzles, whereas the

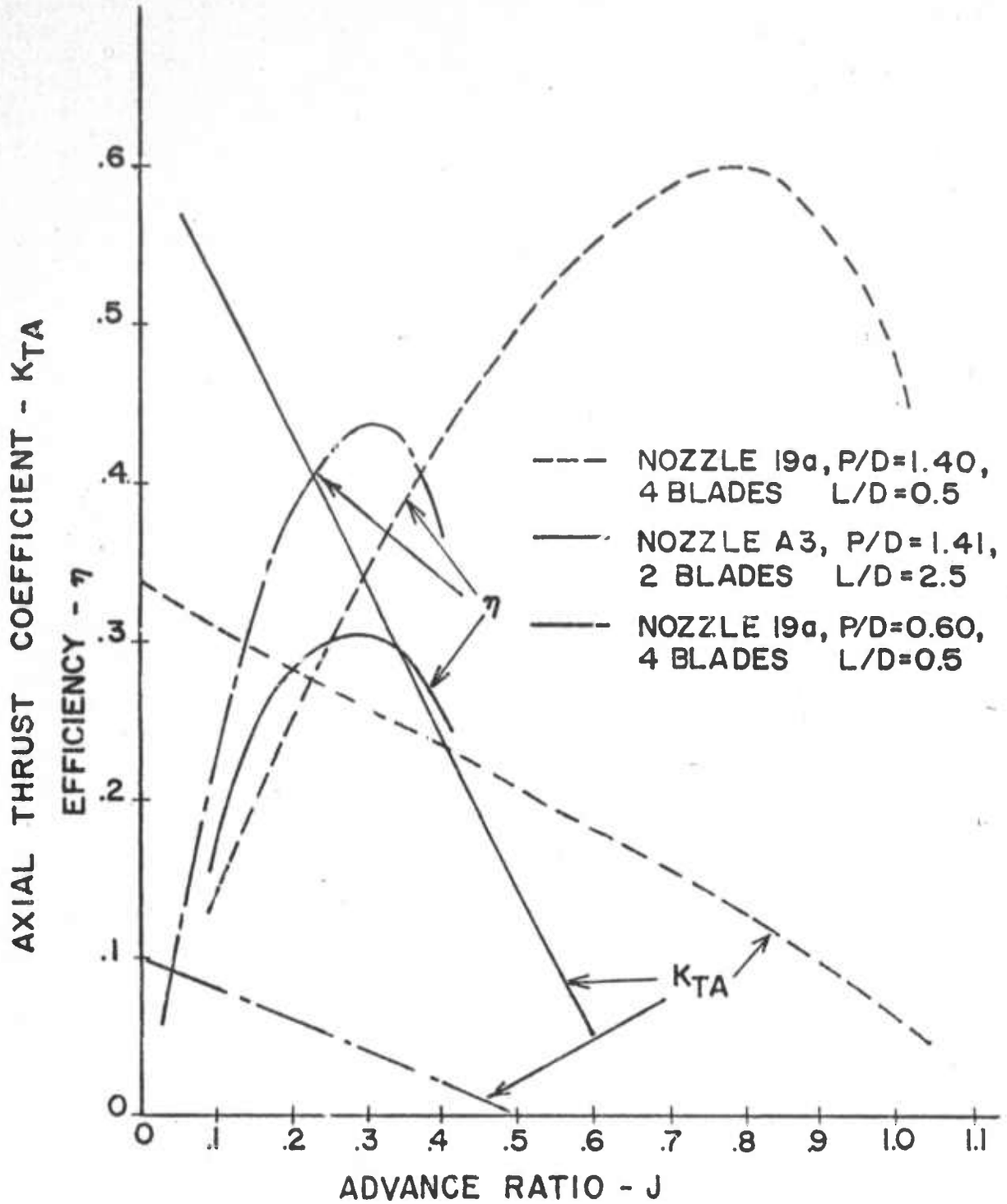

Fig.24 Comparison of the Axial Thrust and Efficiency of the Wake Steering Nozzle with a Conventional Nozzled Propeller

WSN design has not yet been optimized. The lower efficiency is also due to the limitation of the experimental facility, parti--cularly the propellers which had a blade profile opposite that of most conventional propellers. The blades have a sharp leading edge and blunt trailing edge. The blunt trailing edge would tend to produce a turbulent wake, thus lowering propeller efficiency. Higher efficiencies could probably be obtained by testing larger diameter nozzles where more propeller types are commercially available and manufacturing tolerances can be more easily control--led. In addition, the WSN was tested with a two bladed propeller whereas the propellers used in 19a were four bladed. The four bladed propeller would tend to increase propulsive efficiency by minimizing the unsteady flow. WSN efficiency could also likely be increased by further streamlining the nozzles and supporting struts, thus increasing K_{TA}.

Significant differences in axial thrust coefficient are shown in Fig.24. The axial thrust coefficient of the WSN is higher at lower advance ratios but decreases more rapidly with advance ratio than nozzle 19a. The increased axial thrust at low advance ratios could be due to differences in propeller type. Kaplan type propellers which have a wider and flatter blade near the propeller tip were used in 19a. The higher thrust could also be due to the fact that flow through the more divergent WSN tends to separate circumferentially from the inside trailing

edge. The resulting high pressure in the separated region would act to increase the WSN axial thrust coefficient. This separated flow would also increase the drag force, contributing to the rapid decrease in K_{TA} with advance ratio. Another factor causing the rapid decrease in K_{TA} is the larger length to diameter ratio L/D of the WSN. Van Manen and Oosterveld found that the axial thrust and efficiency of nozzled propellers rapidly decreased with length due to increased nozzle drag.[4] This was particularly evident when the nozzle was lightly loaded (low K_{TA}, high J).

At the present stage of development, it appears that the long highly divergent nozzles are an inherent part of the WSN design required in order to develop large radial thrusts for steering. These same parameters tend to decrease its efficiency and effective range of advance ratios as a forward thruster. Consequently, further development and optimization of the WSN should be directed towards minimizing shroud length and divergence while maintaining comparable steering characteristics.

4.2 An Evaluation of the Steering Effectiveness of the WSN

The steering forces developed by movable control surfaces, such as rudders and tiltable shrouds, are usually represented in nondimensional form as lift and drag coefficients by dividing the forces by a term containing rudder area and

fluid velocity. The steering characteristics of different control surfaces can then be compared by simply comparing their representative lift and drag coefficients. The WSN steering force, being a function of propeller thrust, is nondimensionalized by dividing the steering force by a term containing the propeller diameter and rotational speed and therefore a direct comparison is not possible. However, a comparison of the WSN and a conventional control surface is possible for a specific vessel since the propeller thrust and fluid velocity are related through the vehicle dynamics.

The steering characteristics of the WSN are evaluated by comparing it to the tiltable shroud used in the DSRV. This comparison is made by means of computer simulations of the equations of motion of the DSRV given in Reference 17. These were simplified in Reference 18 by considering only motion in the horizontal plane. It is, however, assumed that the vehicle is submerged during all maneuvers in the simulation.

Nozzle A3 with propeller No.4 was chosen on the basis of maximum steering ratio K_{TR}/K_{TA} subject to the constraints of efficiency, size and propeller speed. The WSN used in the simulation had a diameter D of .82 meters and length to diameter ratio L/D of 2.5 giving it a greater area overall than the tiltable shroud which has a diameter of 1.85 meters and L/D ratio of 0.31. The procedure in selecting this WSN is given in Reference 18.

The DSRV equations, together with the equations for tiltable shroud propeller and WSN were programmed on the IBM System 360 computer using CSMP.(19)

Three types of maneuvers were simulated; a full 360° turn, a 90° accelerating turn and a 90°decelerating turn. The results of the 360° turn are shown in Fig.25. The 360°turn or turning circle mareuver is a standard comparative maneuver for marine vessels and is a steady state or constant velocity maneuver.(18) The tiltable shroud was deflected a maximum amount which is also standard for this maneuver. The accelerating and decelerating turns are not standard maneuvers. They were chosen because they are considered to reflect the dynamic maneuvering characteristics of the steering devices. In the accelerating turns, the submersible is accelerated from rest by a constant vehicle axial thrust. In the decelerating turns, the submersible is decelerated from a near maximum cruise velocity of 1.85m/sec by adjusting propeller speed to maintain a near zero axial thrust on the submersible. The simulation was halted in both cases after the submersible had achieved a 90° change in yaw angle. The results for the accelerating and decelerating turns are shown in Figs. 26 and 27 respectively. The numbers in brackets represent the position of the vessel in the axis system at the completion of the 90° turns. The time to complete each maneuver is also given in the figures.

In the case of the standard turning circle maneuver,

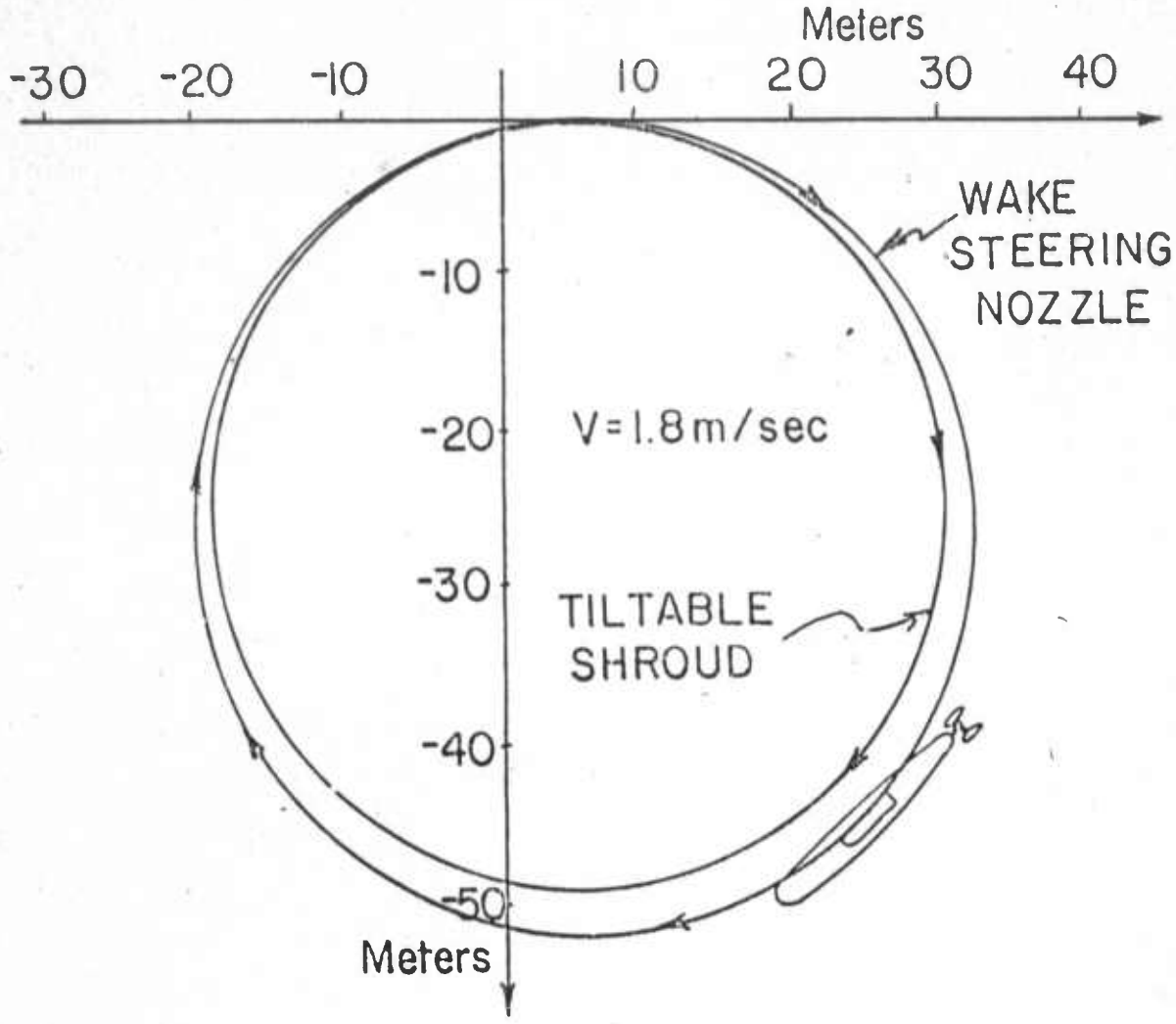

Fig.25 Turning Circle Simulation of DSRV Comparing WSN and Tiltable Shroud

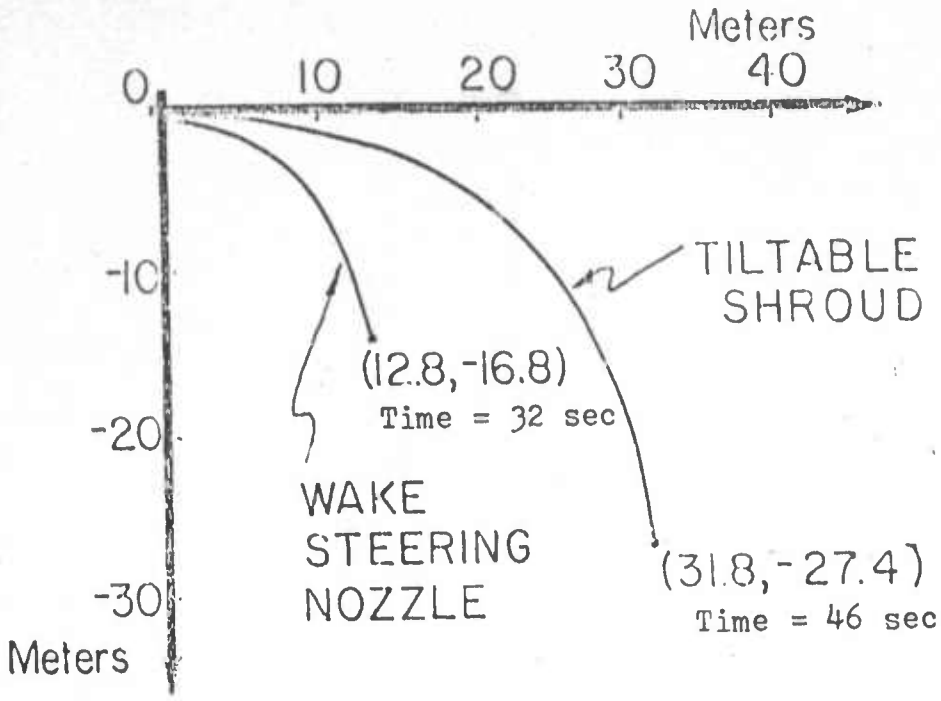

Fig.26 Simulated 90° Accelerated Turn Comparing WSN and Tiltable Shroud

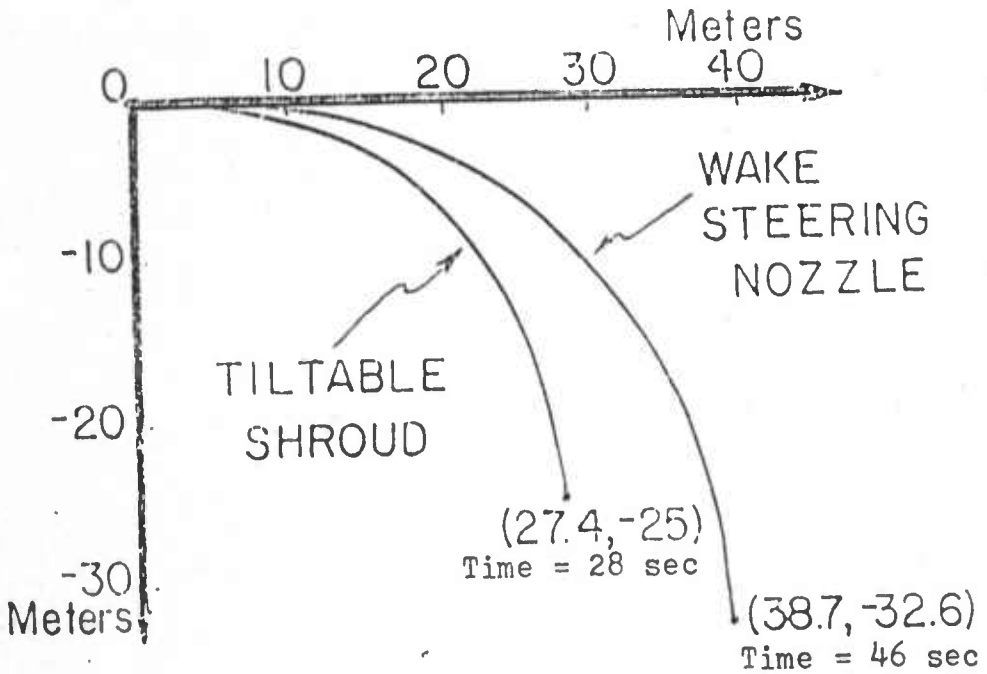

Fig.27 Simulated 90° Deccelerated Turn Comparing WSN and Tiltable Shroud

the performance of the two steering devices is about the same. The accelerating and decelerating turns, however, reveal noticeable differences with the WSN outperforming the tiltable shroud in the accelerating turn but performing less effectively in the decelerating turn. This is to be expected since the high propeller - nozzle thrust of the accelerating turn creates a comparatively high WSN radial or steering thrust while the high forward velocity and low propeller-nozzle thrust of the decelerating turn favor the tiltable shroud.

It should be pointed out that the steering effectiveness of the WSN could be improved by choosing a larger diameter WSN. For example, using a 1 meter diameter nozzle as opposed to the .820 meter diameter nozzle used, increases steering effectiveness K_{TR-A} by about 15% according to the analysis of Reference 18. However, this is done at a sacrifice of a larger shroud size and a lower axial thrusting efficiency.

4.3 A Proposed System for Hovering Control

The proposed use of two WSN, one mounted fore and the other aft, was introduced in Section 1 and is illustrated in Fig.3. This system has the potential capability of replacing the existing thruster-steering system for a submersible such as the DSRV, which has a main propeller, tiltable shroud and

four ducted thrusters.

The arrangement is capable of generating independent forces and moments through cancellation of the axial thrust generated by the two opposing WSN. The resulting thrust cones generated by operating in this configuration are shown in Fig. 28. By reversing the propeller on the front WSN during cruising, a push pull type of thrusting is possible.

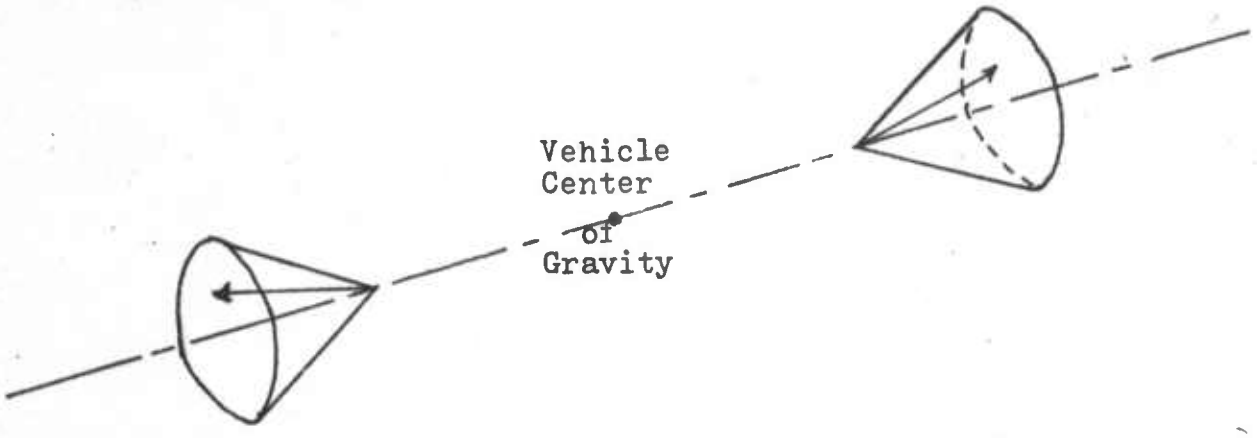

Fig.28 Thrust Vectors Obtained by Mounting WSN on the Tail and Bow of a Submersible

An additional advantage of this system is the potential ability of the WSN mounted on the front of the submersible to produce a radial thrust for both forward and reverse propeller operation. This would improve the submersible steering effectiveness for cruising and for hovering in a current. This would require additional ports on the nozzle fore section.

The magnitude of the radial thrusts and thus the control forces and moments generated are a function of the WSN size, propeller speed and the characteristic thrust coefficients. Considering a WSN having the same dimensions as the nozzle used

in the simulation and using a maximum propeller speed of 5 rev/sec, the maximum radial thrust of this WSN at low advance ratios is about 27000 newtons[18]. This is the same order of magnitude as the maximum thrust of the ducted thrusters on the DSRV[17]. Thus two WSN could produce the same yaw and heave forces as the four ducted thrusters. Because the WSN would be located further from the vehicle center of gravity than the ducted thruster, the pitch and yaw moments generated would be increased an average of about 40% based on the dimensions of the WSN and DSRV.

4.4 Summary

A comparison of the WSN with some conventional propulsion-steering systems has been conducted. The results reveal that one tail mounted WSN is capable of providing submersible steering forces comparible to a tiltable shroud and that mounting another WSN on the front can provide the same forces and moments as the four ducted thrusters, main propeller and tiltable shroud of the DSRV. The chief disadvantage of the WSN is its low propulsive efficiency, particularly at high advance ratios. The efficiency of the WSN can no doubt be increased, as can the range of forward velocity operation of the device, through optimization of the propeller and nozzle design. Shapes other than the arc of a circle need to be investigated. Additional testwork is required to investigate methods of controlling radial force direction and the effect on WSN performance of flows around the nozzle which are not symmetric to the propeller axis.

5. CONCLUSIONS AND RECOMMENDATIONS

This study has demonstrated the feasibilty of the wake steering concept.

The systematic series of static tests revealed that highly divergent nozzles are required to develop the high radial thrusts necessary to maximize the steering effectiveness of the device. However, the wake of the more divergent shrouds showed a tendency to separate when the control port was closed producing an erratic and undesirable radial or steering thrust. This unreliable operation was found to be influenced by nozzle length, propeller type and propeller hub as well. Increasing nozzle length resulted in an increase in WSN reliability. The propellers which were mid-range in the series tested in terms of pitch to diameter ratio were the most reliable. These ranged in P/D ratio from 1.41 to 1.73. However, conclusions as to the effect of propeller pitch are constrained by the fact that the propeller series also differed in other characteristics such as pitch distribution and blade thickness. Including a streamlined hub on the propeller was found to adversely affect WSN reliabilty and a blunt hub was used instead.

A series of nozzles were selected from the static tests to determine the effect of forward velocity on their

operating characteristics. These nozzles were mid-range in terms of reliability and steering thrusts. The results revealed that the reliabilty of the WSN performance was improved compared with the static tests. The radial thrust coefficient also showed an increase with advance ratio indicating an increase in the steering effectiveness of the device with forward velocity. Control of the magnitude of the radial or steering thrust was achieved by locating control ports at different axial locations along the shroud surface.

Based on the static and forward velocity test results, a preliminary comparison of the WSN with some conventional submersible propulsion and steering systems was conducted. The WSN was found to be less efficient as a forward thruster than a conventional nozzled propeller, nozzle 19a. However, the actual numerical differences should not be considered significant since the WSN design has not been optimized, whereas 19a is a highly developed nozzle design. The real significance of the comparison is that it provides direction for future work on the WSN where parameters such as nozzle length and propeller type can be optimized from the point of view of efficiency as well as radial thrust.
In terms of steering effectiveness, the WSN was shown to be as effective as a conventional tail mounted steering device, a tiltable shroud. By mounting a WSN on the bow of a submersible

in addition to one on the tail, the WSN can be considered a potential candidate for replacing the propulsion-steering system of a conventional submersible such as the DSRV which has a main propeller, tiltable shroud, and four ducted thrusters.

Future work on the WSN should be directed towards maximizing the radial thrust of the WSN subject to the constraints of reliable operation and acceptable thrusting efficiency. Other factors must also be taken into consideration The following is a list of recommendations concerning future investigations of the wake steering nozzle:

1) The test work should be conducted on model sizes larger than those used in our test program. This allows the investigation of a much wider range of commercially available propeller types.

2) Propellers having more than two blades should be tested and the effect on performance of propeller hubs be studied more closely.

3) Inside shapes other than the arc of a circle must be investigated. The effect of the outside shape of the nozzle also needs to be considered.

4) Additional test work on the effect of control port location is required.

5) The effect of control port configuration should also be investigated.

6) The effect on WSN performance characteristics of fluid flow at nonzero angles of attack should also be part of any future test program.

LIST OF REFERENCES

1. Taggart,R., "Dynamic Positioning for Small Submersibles", Ocean Industry, August, 1968, pp.44-49.

2. Meiry,J.L., "Space and Deep Submergence Vehicles: Integrated System Synthesis", Journal of Hydronautics, Vol.3, No.2, April, 1969, pp.88-94.

3. Oosterveld,M.W.C., "Wake Adopted Ducted Propellers", Netherlands Ship Model Basin Publication No.345, 1965.

4. Van Manen,J.D. and Oosterveld,M.W.C., "Analysis of Ducted--Propeller Design", Society of Naval Architects and Marine Engineers Annual Meeting, Paper No.13, November, 1966.

5. Van Manen,J.D., "Recent Research on Propellers in Nozzles", Journal of Ship Research, Vol.1, July, 1957, pp.13-46.

6. Morgan,W.B.,"Some Results from the Inverse Problem of the Annular Airfoil and Ducted Propeller", Journal of Ship Research, Vol.13, 1969, pp.40-52.

7. Morgan,W.B. and Caster,E.B., "Comparison of Theory and Experiment on Ducted Propellers", Seventh Symposium Naval Hydro--dynamics, August, 1968.

8. Chaplin,H.R., "A Method for Numerical Calculation of Slipstream Contraction of a Shrouded Impulse Disc in the Static Case with Application to other Axisymmetric Potential Flow Problems", David Taylor Model Basin Report No. 1857, June, 1964.

9. Wozniak,J.J., "A Novel Approach to Submersible Vehicle Pro-
-pulsion, steering and Control", M.S. Thesis, University of New Hampshire, Durham, N.H., June, 1971.

10. Wozniak,J.J., Taft,C.K. and Alperi,R.W., "Wake Steering: A New Approach to Propulsion and Control", Proceedings of the Marine Technology Society, September, 1972, pp.681-698.

11. Clark,J.A., "Design of a Five-Component Water Tunnel Dynamic Balance", M.S. Project, University of New Hampshire, Durham, N.H., January, 1973.

12. Fellows,B.W., "Experimental Investigation of the Static Performance of Propellered Fluidic Nozzles for Thrust Vector Propulsion of Submersible Vehicles", M.S. Project, University of New Hampshire, February, 1974.

13. Abbott,I.H. and Von Doenhoff, Theory of Wing Sections, Dover Publications, New York, N.Y., 1958.

14. Fellows,B.W., Schoenau,G.J. and Taft,C.K., "Propellered Fluidic Nozzles for Thrust Vector Propulsion of Submersible Vehicles", To be presented at the Seventh Cranfield Fluidics Conference, March, 1974.

15. Hudson,R., "Forward Velocity Tests on Wake Steering Nozzles", M.S. Project, University of New Hampshire, Durham, N.H., January, 1974.

16. Comstock,J.P.,(Editor), Principles of Naval Architecture, The Society of Naval Architects and Marine Engineers, New York, N.Y., 1967.

17. Lockheed Missiles and Space Company, "DSRV Model For Analysis", Report No. RV-R-0037A, May, 1968.

18. Schoenau,G.J., "Submersible Maneuvering and Control", Ph.D. Dissertation, University of New Hampshire, Durham, N.H., To be completed in Spring, 1974.

19. IBM, System/360 Continuous System Modelling Program User's Manual, No.GH20-0367-3, October, 1969.